REPORT DOCUMENTATION PAGE

AFRL-SR-AR-TR-05-

0411

1. AGENCY USE ONLY *(Leave blank)*	2. REPORT DATE	3. REPORT T... ...ES COVERED
		01 Feb 2002 - 30 Jun 2005 FINAL

4. TITLE AND SUBTITLE
DETECTION AND STERILIZATION OF ANTHRAX SPORES BY MICROWAVE RADIATION

5. FUNDING NUMBERS
61102F
2301/EX

6. AUTHOR(S)
PROFESSOR LUHMANN JR

7. PERFORMING ORGANIZATION NAME(S) AND ADDRESS(ES)
REGENTS OF THE UNIVERSITY OF CALIFORNIA DAVIS
SPONSORED PROGRAM
118 EVERSON HALL
DAVIS CA 95616

8. PERFORMING ORGANIZATION REPORT NUMBER

9. SPONSORING/MONITORING AGENCY NAME(S) AND ADDRESS(ES)
AFOSR/NE
4015 WILSON BLVD
SUITE 713
ARLINGTON VA 22203

10. SPONSORING/MONITORING AGENCY REPORT NUMBER
F49620-01-1-0481

11. SUPPLEMENTARY NOTES

12a. DISTRIBUTION AVAILABILITY STATEMENT
DISTRIBUTION STATEMENT A: Unlimited

12b. DISTRIBUTION CODE

13. ABSTRACT *(Maximum 200 words)*

The goal of this program is to investigate the ability of microwave and millimeter-wave radiation to detect and destroy biological agents, with a particular focus on anthrax spores. Dry constituents, such as dipicolinic acid (DPA), can be placed within simple waveguide holders and subsequenly probed. Other constituents are available only in liquie suspension, and require use of coplanar waveguide measurement fixtures. DPA has been probed over a frequency range of 8-170 GHz using multiple sample holders over multiple waveguide bands. Although not conclusively verified, testing to date indicate the presence of two relatively broad dielectric resonances at -127 GHz and -155 GHz using the new technique.

14. SUBJECT TERMS			15. NUMBER OF PAGES
			16. PRICE CODE
17. SECURITY CLASSIFICATION OF REPORT	18. SECURITY CLASSIFICATION OF THIS PAGE	19. SECURITY CLASSIFICATION OF ABSTRACT	20. LIMITATION OF ABSTRACT
Unclassified	Unclassified	Unclassified	UL

DOD FINAL REPORT
U.S. Department of Defense Grant No. F49-620-02-1-0114

Sept. 23, 2005

Detection and Sterilization of Anthrax Spores by Microwave Radiation

PRINCIPAL INVESTIGATOR:
Prof. N.C. Luhmann, Jr.
Phone: (530) 752-5414
Facsimile: (530) 754-9070

PROGRAM MANAGER:
Dr. Robert Barker
Air Force Office of Scientific Research

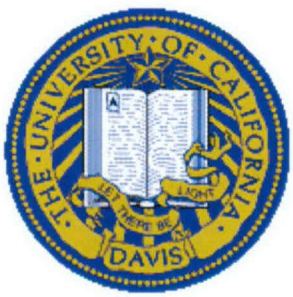

UNIVERSITY OF CALIFORNIA, DAVIS
Department of Applied Science and
Department of Electrical and Computer Engineering

Scientific Staff

Prof. N.C. Luhmann, Jr.: Principal Investigator

Dr. C. W. Domier

Mr. A. Wan

Mr. M. Johnson

Detection and Sterilization of Anthrax Spores by Microwave Radiation

I. Executive Summary

The past and future use of biological agents in warfare and terrorism is of particular concern not only because of recent exposures, but also because their physiological properties make them ideally suited for use as a weapon. Of the numerous biological agents that may be used as weapons, the Working Group on Civilian Biodefense has identified anthrax (*bacillus anthracis*) as one of the most serious of these diseases. The best way to safeguard against anthrax infection is to detect and kill the spores before they have a chance to infect the host. This is not an easy task. Anthrax spores, like those of all *bacillus* bacteria, are designed for survival under extremely harsh conditions.

The goal of this program is to investigate the ability of microwave and millimeter-wave radiation to detect and destroy biological agents, with a particular focus on anthrax spores. The approach taken by UC Davis to identify microwave/millimeter-wave resonances is to first examine major *bacillus anthracis* spore constituents, which would allow for a significant "kill" enhancement by tuning the irradiation source to match the detected resonance. Dry constituents, such as dipicolinic acid (DPA), can be placed within simple waveguide holders and subsequently probed. Other constituents are available only in liquid suspension, and require use of coplanar waveguide measurement fixtures.

DPA has been probed over a frequency range of 8–170 GHz using multiple sample holders over multiple waveguide bands. Transmission resonance dips have been observed at many frequencies; however, the frequency of these dips is observed to move as the depth of the sample holders is changed. Such dips are often the result of destructive interference, where small reflections can effectively null out the signal at the detector leading to a deep but narrow dip in the transmission curve. Conclusively identifying these lines has proven to be extremely time-consuming, as the measurement setups themselves are fraught with spurious reflections and standing wave patterns that considerably complicate the relatively basic S-parameter measurements. After many false starts, we are now able to generate clean setups in each waveguide band. Conclusive identification of dielectric resonances is then made by repetitively measuring the transmission through multiple sample depths. A resonance can be identified by examining those frequency ranges in which the transmission is significantly reduced at all sample depths tested.

Our Ph.D. student is now in the process of retesting DPA over the full available testing range of 8-170 GHz in order to both complete his dissertation research and to fulfill the goals of the AFOSR program. Although not conclusively verified, **testing to date indicate the presence of two relatively broad dielectric resonances at ~127 GHz and ~155 GHz** using this new technique. Data collected and analyzed with this technique will form the basis of a paper to be submitted later this year to *IEEE Microwave and Wireless Components Letters*. In addition to the dry sample testing, test fixtures with a frequency range that extends from 45 MHz to 40 GHz have been developed for liquid samples including biological materials in liquid suspension. The fixtures developed to date have been employed to study the dielectric response of a number of "test" fluids including ethanol and isopropyl alcohol.

Progress on this project was presented at this year's *Electro-Med 2005 Symposium*, which was held in Portland, Oregon on May 15-18, 2005. The most recent results were included in a talk presented at the *Joint 30th International Conference on Infrared and Millimeter Waves and 13th International Conference on Terahertz Electronics (IRMMW-THz)*, which was held in Williamsburg, Virginia on September 19-23, 2005.

II. Background and Motivation

A. Motivation

The past and future use of biological agents in warfare and terrorism is of particular concern not only because of recent exposures, but also because their physiological properties make them ideally suited for use as a weapon. Of the numerous biological agents that may be used as weapons, the Working Group on Civilian Biodefense has identified a limited number that could cause disease and deaths in sufficient numbers to cripple a city or region. Anthrax (*bacillus anthracis*) is one of the most serious of these diseases. Anthrax organisms can cause infection in the skin (cutaneous anthrax), gastrointestinal system (gastrointestinal anthrax), or the lungs (inhalation anthrax). If untreated, anthrax in all forms can lead to septicemia, hemorrhagic meningitis, and death. The case fatality ratio for patients with appropriately treated cutaneous anthrax is usually <1%, but for inhalation or gastrointestinal disease it can exceed 50%.

The possibility of creating aerosols containing anthrax spores has made *B. anthracis* a chosen weapon of bioterrorism. Several powers may have the ability to load spores of *B. anthracis* into weapons. Domestic terrorists may develop means to distribute spores via mass attacks or small-scale attacks at a local level. As an agent of biological warfare it is expected that a cloud of anthrax spores would be released at a strategic location to be inhaled by the individuals under attack. Spores of *B. anthracis* can be produced and stored in a dry form and remain viable for decades in storage or after release

The best way to safeguard against anthrax infection is to detect and kill the spores before they have a chance to infect the host. This is not an easy task. Anthrax spores, like those of all Bacillus bacteria, are designed for survival under extremely harsh conditions. Mature spores have no detectable metabolism, a state that is described as **cryptobiotic**. They are highly resistant to environmental stresses such as high temperature (some endospores can be boiled for several hours and retain their viability), irradiation, strong acids, disinfectants, etc. Although cryptobiotic, they retain viability indefinitely such that under appropriate environmental conditions, they germinate into vegetative cells. Endospores are formed by vegetative cells in response to environmental signals that indicate a limiting factor for vegetative growth, such as exhaustion of an essential nutrient. They germinate and become vegetative cells when the environmental stress is relieved. Hence, endospore-formation is a mechanism of survival rather than a mechanism of reproduction.

In cross section (see Fig. 1), *Bacillus* spores show a more complex ultrastructure than that seen in vegetative cells. The spore protoplast (core) is surrounded by the core (cell) wall, the cortex, and then the spore coat. Depending on the species, an exosporium may be present. The core wall is composed of the same type of peptidoglycan as the vegetative cell wall. The cortex (Cx) is composed of a unique peptidoglycan maintain the dehydrated state of the spore (~15% water) and facilitate germination in the host. The outer spore coat represents 30-60% of the dry weight of the spore. Inside the cortex, spore contents (Sc), including DNA, are dehydrated with a large amount of calcium-bound dipicolinic acid (DPA) present. DPA imparts a high degree of heat resistance to spore contents. The spore coat (Ct) is composed of heavily crosslinked, keratin-like proteins with an unusually high content of cysteine and of hydrophobic amino acids, which protect the spore from extreme chemical conditions and proteolysis.

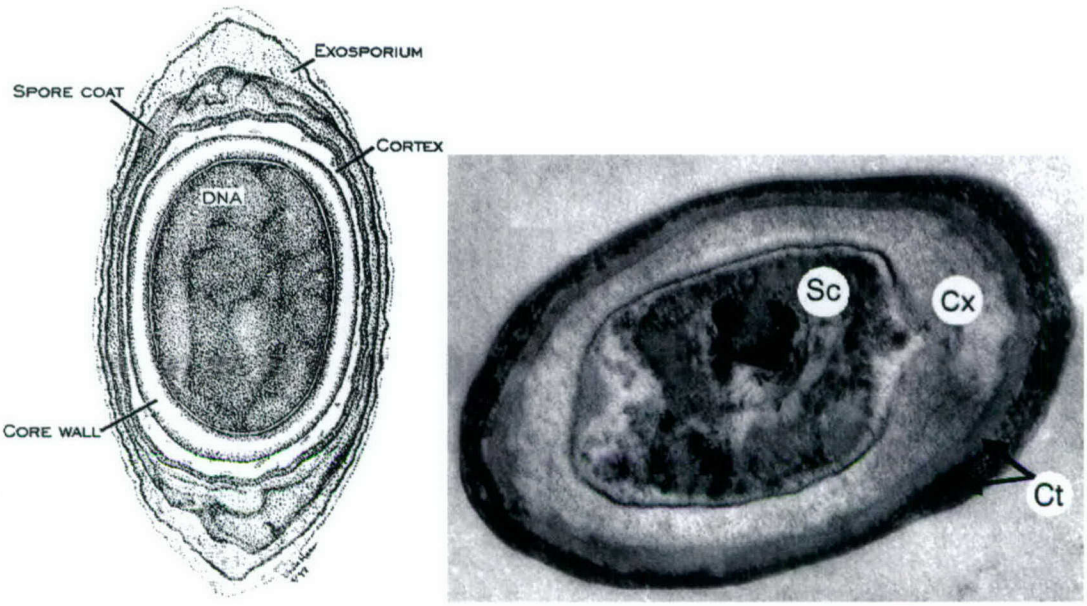

Fig. 1. Drawing of a cross-section of a *Bacillus* endospore by Viake Haas, University of Wisconsin (shown left), and photograph of a bacillus subtillus spore (shown right).

The goal of this AFOSR program is to investigate the ability of microwave and millimeter-wave radiation to detect and destroy biological agents, with a particular focus on anthrax spores. The approach taken by UC Davis to identify microwave/millimeter-wave resonances is to first examine major *bacillus anthracis* spore constituents that would allow for a significant "kill" enhancement by tuning the irradiation source to match the detected resonance. Dry constituents, such as dipicolinic acid (DPA), can be placed within simple waveguide holders and probed. Other constituents are available only in liquid suspension, and require use of coplanar waveguide or microstrip-based measurement fixtures.

B. Background

The dielectric effect on polar water molecules has been known since 1912 [1], with the effectiveness of microwaves for sterilization well established by numerous studies [2-4]. The exact nature of the sterilization effect, and whether it is due solely to thermal effects (arising from the dielectric effect on polar water molecules) or to a 'microwave effect', has been a matter of controversy for decades.

Microwave irradiation experiments have generally fallen into two categories: (1) controlled temperature experiments, and (2) dry. In controlled temperature experiments by Welt [5], microwave radiation was observed to produce an identical level of inactivation of microbial cells and spores as that by conventional heating. A subsequent study by Vaid and Bishop [6] showed that low frequency microwave radiation of bacterial endospheres caused disruption and fragmentation of endospore DNA, with the damage due primarily to the thermal heating of water molecules within the spore. The effect upon DPA was deemed negligible at these frequencies.

In the second type of experiment, studies have shown that in the absence of water or moisture, biocidal effects of microwaves are severely diminished, or require considerably longer exposures [7]. This was generally taken as evidence that nonthermal microwave effects did not exist, as water is the primary medium by which microwaves are converted to heat. The

experiments may simply be indicating, however, that the wrong frequency is being used for targeting 'dry' bacteria and spores.

Most researchers have concluded that the microwave effect, if it exists, is indistinguishable from the effects of external or thermal heating. Kakita demonstrated in 1995, however, that microwaves are capable of extensively fragmenting viral DNA, something that heating to the same temperature did not accomplish [8]. This experiment consisted of irradiating a bacteriophage PL-1 culture at 2.45 GHz and comparing this with a separate culture heated to the same temperature. The DNA was mostly destroyed (see Fig. 2), a result that does not occur from heating alone. In the Kakita experiment, the survival percentage was approximately the same whether the samples were heated or irradiated with microwaves, but evaluation by electrophoresis and electron microscopy showed that the DNA of the microwaved samples had mostly disappeared. Vaid and Bishop reported similar results in 1998 [6]. They observed that, with respect to the disruption of spores at a given temperature, microwave radiation has a greater effect than conventional heating. Spores of clostridium sporogenes, for example, showed clear signs of disruption to their structure after microwave heating at 100°C for 8 minutes, while a similar exposure to boiling left them visibly unchanged. This led them to conclude that microwaves involve a different mechanism on bacterial spores from that of conventional heating such as boiling or autoclaving. While conventional methods for destroying cells often rely upon the generation of external pressure, the spore fragmentation observed is presumably the result of an explosion of internal pressure generated within the core.

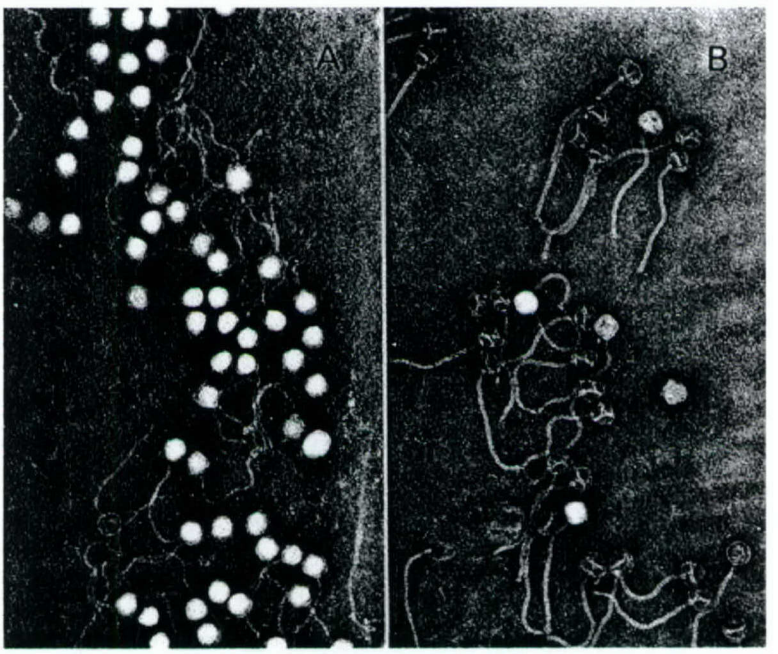

Fig. 2. The Image above shows bacteriophage PL-1 before (left) and after (right) irradiation with microwaves. The DNA has mostly been destroyed, a result that does not occur from heating alone. These photos are borrowed from Kakita *et al.* [8].

Study of the 'microwave effect' continues today, with promising results. Results from a more recent study by Kakita [10] are plotted in Fig. 3, showing bacterial survival as a function of 2.45 GHz microwave exposure time. At a recent workshop entitled *Biocomplexity VI: Complex Behavior in Unicellular Organisms*, held at Indiana University on May 12-16, 2004, results were

presented of a University of North Carolina study on variable frequency microwave irradiation of *bacillus subtilis* spores. An accelerated kill rate was observed over dry heat in a convection oven, although the kill mechanism was not identified.

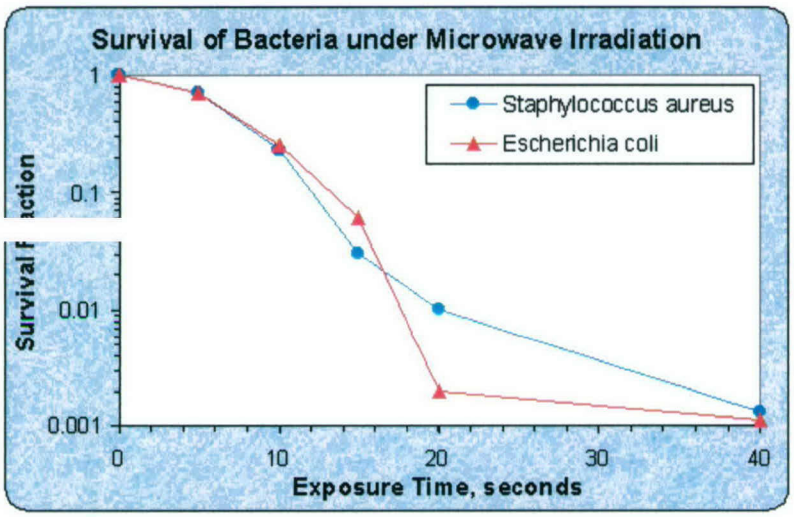

Fig. 3. Results of 2.45 GHz irradiation of two bacteria, *S. aureus* and *E. coli*. The death curves exhibit classic exponential decay with an apparent shoulder, as well as a possible second stage. These curves are based on data from Kakita *et al.* [10].

Theoretical work by Purdue University opened up the possibility of low-energy absorption resonance in DNA at microwave and millimeter-wave frequencies [11]. The microwave and millimeter-wave region is a difficult region for spectroscopic measurements, since measurement errors have plagued numerous previous biological studies resulting in considerable confusion and doubt. Plotted in Fig. 4 are *bacillus anthracis* data by Dr. Jing Ju of the Stevens Institute of Technology [12,13]. The data shown here correspond to different film thicknesses, as measured at normal incidence. Note the apparent "negative" absorption that arises from multiple reflection interference.

More successful was experimental work by the Army Research Laboratory [14,15] and University of Virginia [16-18], which demonstrated that Bacillus subtilis DNA exhibits *phonon modes* with resonances in the 0.1-10 THz frequency range. Three such resonances have since been directly measured, with resonance frequencies of 253, 418 and 1037 GHz, as reported by Dr. E.R. Brown [19, 20]. These are relatively weak resonances, however, and appear to be the result of single-bioparticle electromagnetic resonances and occur at frequencies where high power millimeter-wave sources are not readily available for irradiation use.

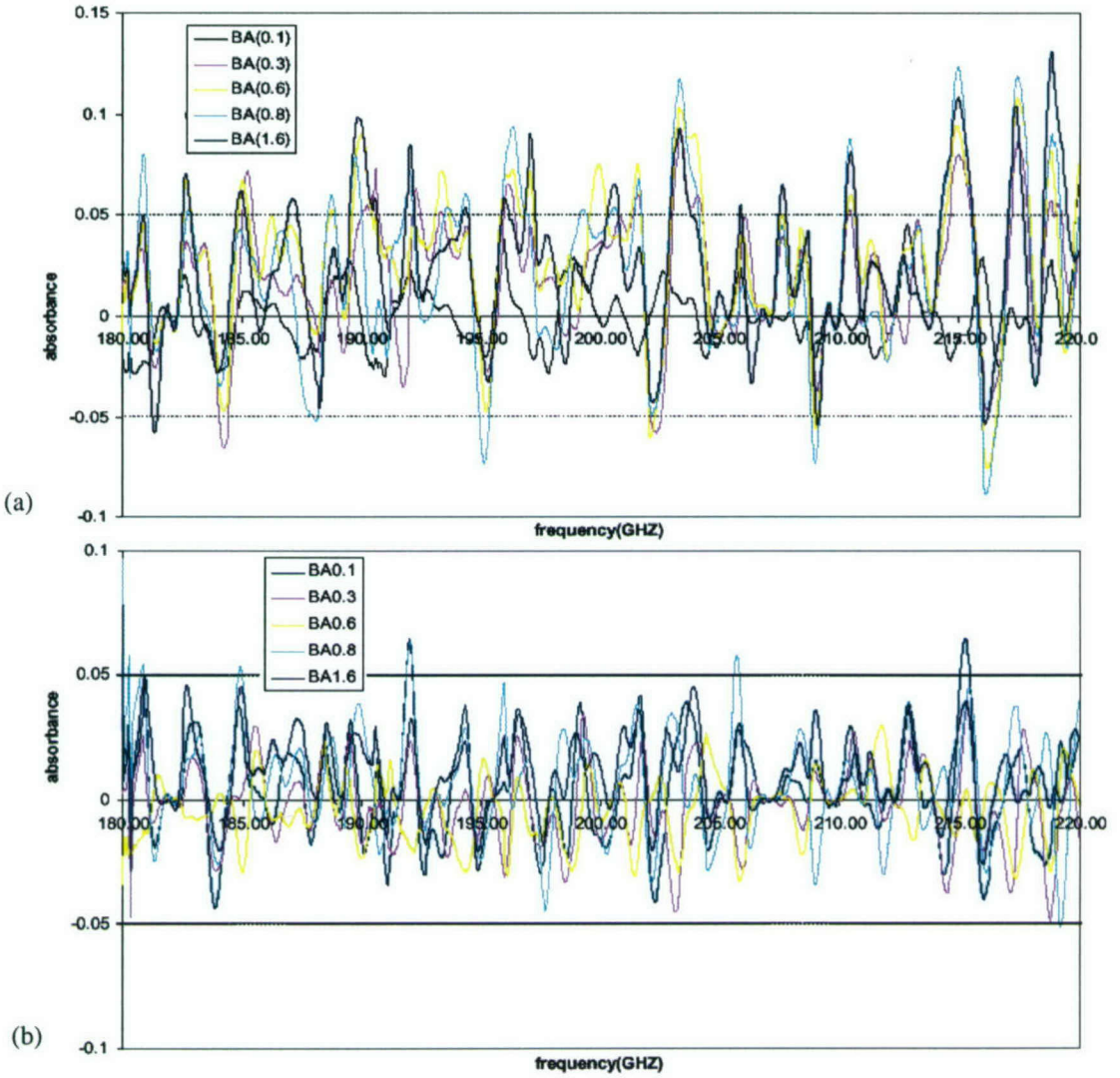

Fig. 4. Absorption features of bacillus anthracis film at (a) normal incidence, and (b) tilted at 15° [from 12].

Of more interest to this AFOSR sponsored program, however, are the results of calculations by van Zandt and Saxena on the vibrational spectrum of a dissolved DNA polymer that predict the existence of plasmon modes at microwave frequencies [11]. The frequency of these plasma modes is dependent upon the type and orientation of sample DNA films, but their predictions are for a series of resonances at 10.5, 21.0, 31.5, ... GHz. These theoretical predictions provide strong motivation for the search for microwave resonances for which suitable high power irradiation sources are more easily obtained.

III. Spore Component Characterization Activities

A. Spore Components and Characterization Overview

To evaluate the potential of microwave radiation for detecting and destroying anthrax spores, we have focused on independently characterizing the dielectric response of a number of purified compounds that represent the major components of anthrax spores. The compounds present as major components of spores are:

1. Dipicolinic acid (DPA) and calcium – present in inner spore contents.
2. Proteoglycans (commercially available; gram positive) – similar to cortical layer
3. Filamentous keratin – (similar to outer protective layers)
4. DNA (genomic and circular plasmids)

DPA is readily available in dry form, and can be placed within simple waveguide structures and thus probed. Its purpose is to protect the spore DNA from heat and radiation damage. The remaining constituents are all available in liquid suspension form, and can be probed in suitable liquid sample test fixtures developed in this AFOSR sponsored program.

Also available for testing are Bacillus spore test strips, available from Raven Biological Laboratories (see Fig. 5, left), which can be incubated to grow a sufficient quantity of spores for testing. An extended spore strip can be laid out over a suitable transmission line (developed for liquid sample testing) and probed to determine its dielectric response at frequencies $\leq$ 40 GHz. Another possible test structure is a micro-pillar array, fabricated by MicroEnergy Technologies, Inc (see Fig. 5, right). The size and shape of the pillars are designed to trap particulates of a certain size with high efficiency. The idea here would be to capture bacillus subtilis test spores in the micro-pillars, and then place the micro-pillar strips into a specially designed transmission line test fixture for study. If successful, this would allow use in a possible anthrax field detection system and is a possible subject for future study.

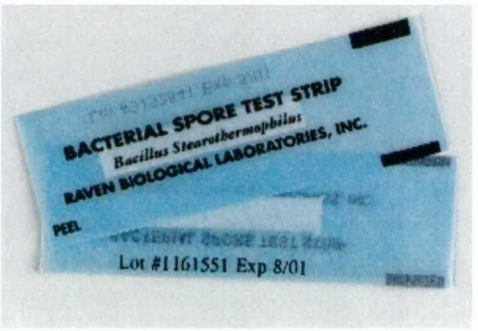

Bacillus subtilis - ATCC # 9372. For use in Ethylene Oxide (600 mg/L), Dry Heat Sterilization (calculated at 160°C), and formaldehyde fumigation. After exposure to sterilant, incubate strips at 35°C. Populations of strips are typically from 1.0 X 10^6 to 4.0 X 10^6.

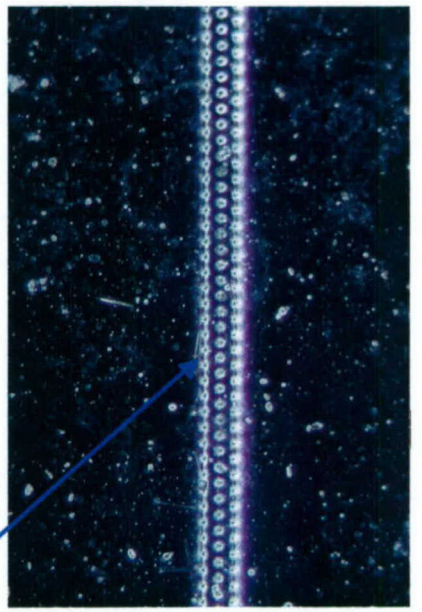

Fig. 5. Arrangement for anthrax and pathogen absorption spectroscopic measurements.

Before our measurements could commence, we were required to write up an Operational Safety Procedure (OSP), describing the protocols for safe handling, use, control measures and experimental procedures associated with this experiment. This OSP was submitted to and approved by the Dept. of Environmental Health & Safety at UC Davis, and is provided in the following.

1. Motivation and Purpose of this Research

The broad aim of this project is (1) investigate the microwave spectroscopic properties of bacillus subtillus, a close relative of the bacillus anthrax. (2) Identify the presence of any dielectric resonances. (3) Investigate the possibility of applying coherent microwave radiation, whose frequency matches that of the dielectric resonance, in an effort to cause a breakdown in the internal structure of the bacillus.

It should be noted here that there are no plans to work with the highly dangerous bacillus anthrax, but rather to investigate its more common and harmless "cousin" the bacillus subtillus with which it shares a number of common molecular structures.

The motivation for this project is as follows. It has been identified by a number of research laboratories, both in this nation and across the world, that the bacillus anthrax is an extremely hardy organism while in its spore state. While it is theoretically possible to "cook" the spore through the application of high power microwaves (which couple to a dielectric resonance in water molecules), the extremely low water content of the spores renders this unfeasible. Our hope is to find a resonance in one of the key molecular structures that make up the bacillus. Then, apply microwave power at this resonance to break down its internal structure and "kill the organism" at power levels much reduced from that required for "cooking." As proteins and other biological molecules have been found to have rather large, distinct dielectric properties in the microwave regime, this approach makes this an attractive option to investigate.

This Operational Safety Procedure (OSP) covers the first two stages of this investigation. A separate OSP will be submitted, should the first two stages result in a clear identification of microwave resonances. The biochemical materials we are interested in using include: Dipicolinic Acid (main substance in spores), subtillus DNA, subtillus spores, Keratin, and Proteoglycan. The dielectric properties of these materials will be studied using a Hewlett-Packard 8510C Vector Network Analyzer. Our group is fortunate to have two such instruments available. The instrument located in 1104 EU-III is capable of covering a frequency range of 10 MHz to 26.5 GHz, and the unit in 1209 EU-II from 10 MHz to 40.0 GHz. Testing at higher frequencies is possible through the use of frequency extenders, which in principle can extend our measurements as high as 110 GHz.

2. Laboratory Location

1104 EU-III and 1209 EU-II. Samples will be prepared within a ventilated fume hood in 1104 EU-III. Samples will be tested using network analyzers in 1209 EU-II and 1104 EU-III.

3. Participants

The research will be conducted by researchers Drs. Eric Landahl and Calvin Domier and graduate student researcher Xiang Wan under the supervision of Prof. N.C. Luhmann, Jr.

4. Biochemical Materials to be used

The materials are all components of Bacillus subtillus, classified as Biosafety Level 1. These materials include Dipicolinic Acid, Subtillus DNA, Subtillus Spores, Keratin, and Proteoglycan.

5. Precautions for Safe Handling, Use and Control Measures

The following general measures for the safe handling and use of the biochemical materials, as obtained from MSDS data sheets provided by the suppliers of these materials.

Material Released/Spill: Sweep up material & package for safe pick up by Environmental Health and Safety (EH&S) personnel.

Precautions-Handling/Storing: Biochemical material samples will be stored in the original containers, which are to be kept tightly closed and stored within a ventilated fume hood. When handling liquid products (although only powdered samples are presently planned to be employed), secondary protective

containers must be used for carrying. Avoid contact with eyes, skin and clothing. Avoid breathing dust. Avoid contact with strong acids and bases. Keep away from oxidizing materials.

Respiratory Protection: None required where adequate laboratory ventilation exists. However, Fisher Scientific Facemasks (99% bacterial filtration efficiency) will be worn when preparing samples for testing as an added precaution.

Ventilation: Use fume hood and laboratory ventilation.

Protective Clothing: Laboratory coat required – Fisher Scientific White Night Lab Coats made of polypropylene with three front snaps.

Protective Gloves: Required - Fisher Scientific Model 19-041 Series powdered vinyl medical gloves.

Eye Protection: Fisher Scientific PVC goggles will be worn when preparing or handling samples.

Emergency/First Aid Procedures:

Ingestion: Do not induce vomiting. If conscious, give large amounts of water.

Inhalation: Remove to fresh air. Give CPR/Oxygen if needed. Prompt action is essential.

Skin Contact: Immediately flush with plenty of water for 15 minutes.

Eye Contact: Immediately flush with plenty of water for 15 minutes. Obtain medical attention in all cases.

Hazardous Waste Storage/Disposal Methods: All wastes are to be decontaminated with a liquid bleach solution, after which they can be drain disposed.

6. Experimental Procedures

Laboratory Access and Laboratory Use: Access to the laboratory is limited or restricted at the discretion of the laboratory director when experiments or work with specimens are in progress. Eating, drinking, smoking, handling contact lenses, applying cosmetics, and storing food for human use are not permitted in the work areas. Persons who wear contact lenses in laboratories should also wear goggles or a face shield. All persons should wash their hands before leaving the laboratories.

Sample Preparation: Turn on HP 8510 network analyzer and recalibrate as required. Wearing protective gloves, lab coat, safety mask and face shield, carry the appropriate sample container containing the biochemical material to the bench top designated for this experiment. Open the sample container and pour measured amount into the waveguide short, taking care to fill to a predetermined depth. Remove waveguide short from bench top and attach to HP 8510 network analyzer. Protective gloves, lab coat, safety mask and face shield may then be safely removed while testing. Persons wash their hands after handling the materials and removing gloves.

Sample Storage: Wearing protective gloves, lab coat, safety mask and face shield, disconnect the waveguide short containing the biochemical sample from the HP 8510 network analyzer and transport the waveguide short to the designated bench top. Pour the contents of the waveguide short back into the original sample container. Protective gloves, lab coat, safety mask and face shield may then be safely removed once the container is tightly sealed and placed back within the ventilated fume hood. Note that the samples may be continuously reused and retested as needed, with disposal taking place only after all measurements have been completed.

Bench Top Clean up: Work surfaces are decontaminated at least once a day using a liquid bleach solution, and after any material spill.

B. Dry Sample Measurements

Dry sample measurements of DPA are measured by placing the sample into a sample holder (empty waveguide of a calibrated length), and then measuring the transmission and/or reflection properties of the sample as a function of frequency. HP 8510 Vector Network Analyzers are employed at frequencies up to 40 GHz, while scalar network analyzer setups are employed from 40 to 170 GHz.

B.1. One-Port (S_{11}) Vector Analyzer Data from 8 to 40 GHz

The HP 8510 network analyzer is controlled by a PC running LABVIEW data acquisition software. The first measurements involved simple test structures, as shown below in Fig. 6 and schematically in Fig. 7. A one-port measurement technique was employed, in which an HP8510 vector network analyzer measures the reflected amplitude and phase of a shorted waveguide test structure with and without the presence of the sample material within the test structure. Here, the sample holder is oriented vertically such that gravity forces the powdered sample to rest in the bottom of the test structure next to the waveguide short. Data collected in this way are then transferred to a nearby PC for storage and analysis.

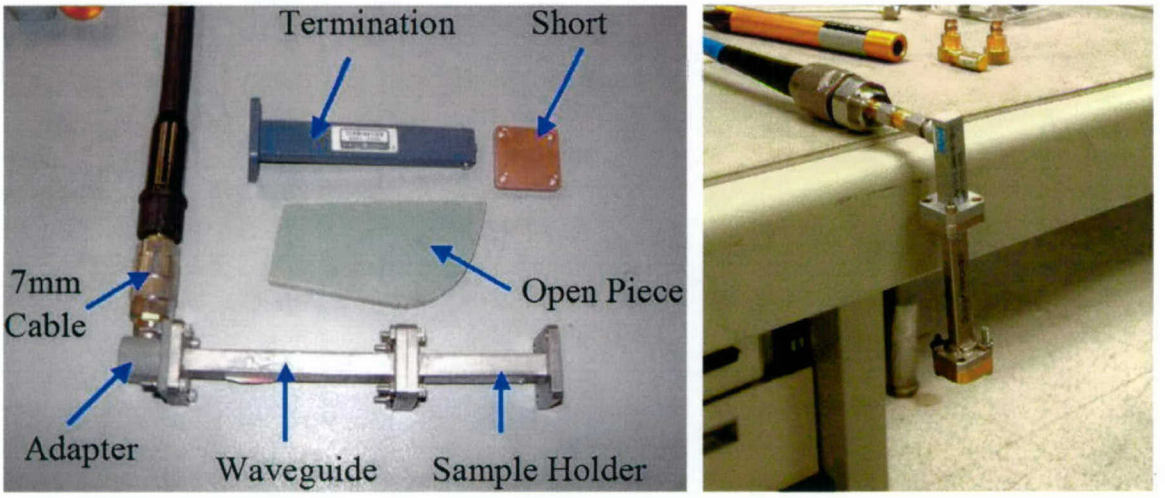

Fig. 6. Photograph of microwave components employed for one-port dielectric response measurements in Ku-Band (left), and Ka-Band (right).

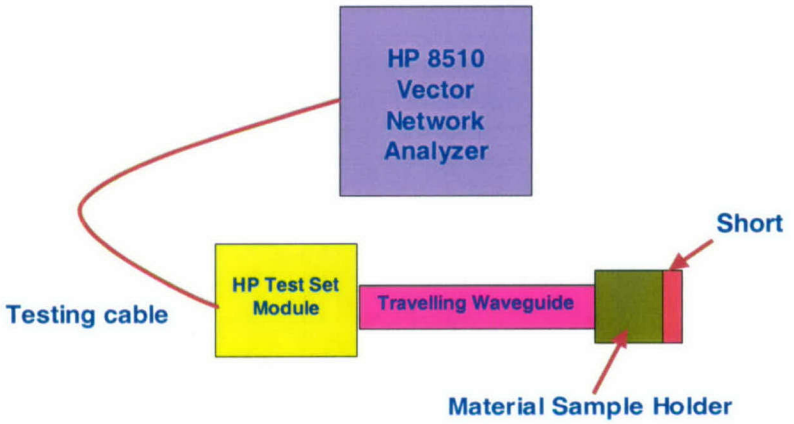

Fig. 7. Schematic of the configuration for an S_{11} one-port measurement

The procedure employed is straightforward. The system, including the empty sample holder, is calibrated to remove cable and connector losses. Varying sample amounts are then placed into the sample holder, and the reflection coefficient of the sample holder is then measured (as compared to the "calibrated" results of the empty holder). This helps ensure that detected resonances are "real" (i.e., a property of the anthrax constituent) and not simply a fixture artifact by verifying that the resonance frequency is not amount dependent.

The first dielectric characterization measurements were made over a 7-12 GHz frequency range with a network analyzer setup at Stanford University. These data were taken during the period while the UC Davis test setup was being put together and the OSP written up. The material tested and shown below is DPA, one of the major constituents of both *B. anthracis* and *B. subtillus* spores. Other than the known analyzer glitch at ~11 GHz, due to internal switching within the analyzer, there was no sign of a strong dielectric resonance over this frequency range. Nonetheless, this demonstrated the strong promise of the accuracy of the basic measurement technique.

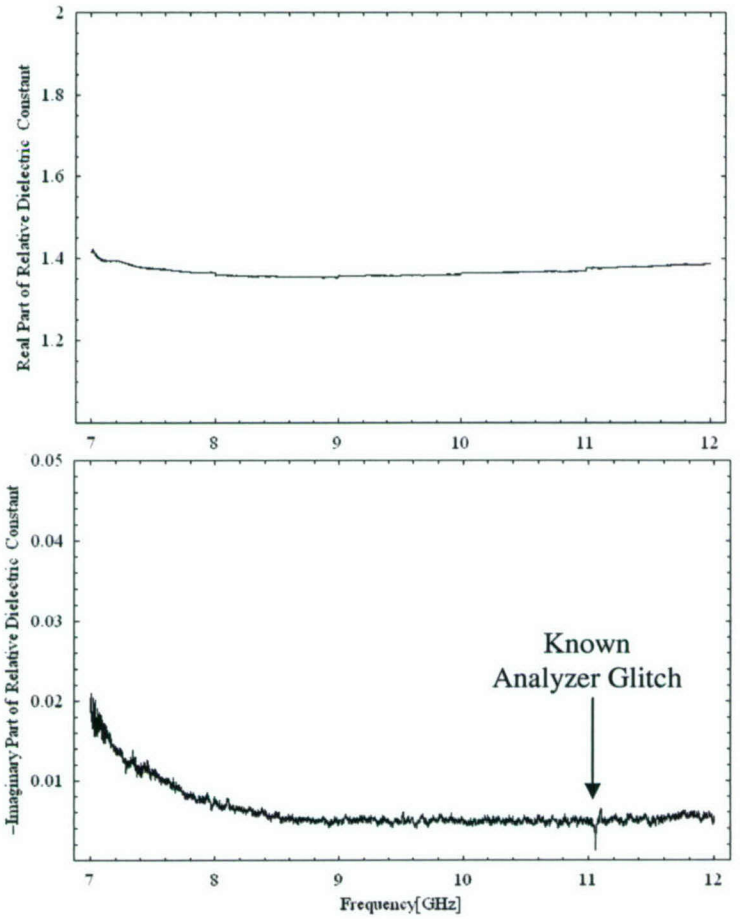

Fig. 8. Reconstructed real (top) and imaginary (bottom) parts of the dielectric constant of DPA, as obtained from S_{11} network analyzer measurements.

We follow with the Ku-Band (12.4-18.0 GHz) results obtained with DPA. Plotted in Fig. 9a (upper left) is the post-calibrated reflection from the empty sample holder. Plotted in Figs. 9b-d are the return loss measurements from the sample holder containing differing depths of DPA within it, ranging from little (1.8 cm), half (5.3 cm) to full (11 cm). The motivation behind taking multiple depth measurements is clearly seen from the data below. A number of apparent resonances appear in each plot, with depths ranging from 1 to > 8 dB. We note, however, that not only does the "resonance" attenuation change as a function of sample depth, but so does the "resonance" frequency leading to the conclusion that these are simply measurement artifacts. The most likely cause of these artifacts is the presence of multiple reflections that form standing waves within the sample holder. The non-unity refractive index of the test sample results in (a) a

finite reflection from the air-sample interface, and (b) a phase-delayed and reduced amplitude reflection from the waveguide short at the bottom of the sample holder. Acting together with other reflection sources such as the coaxial-to-waveguide adapter which connects the sample holder to the HP 8510 network analyzer, forms a complicated interference pattern which at particular frequency values results in destructive interference of the reflected wave and a "dip" in the measured S_{11} amplitude. Note that if these were true absorption resonances, the frequency location of the S_{11} resonance would remain fixed while the resonance depth would increase with increasing sample amount.

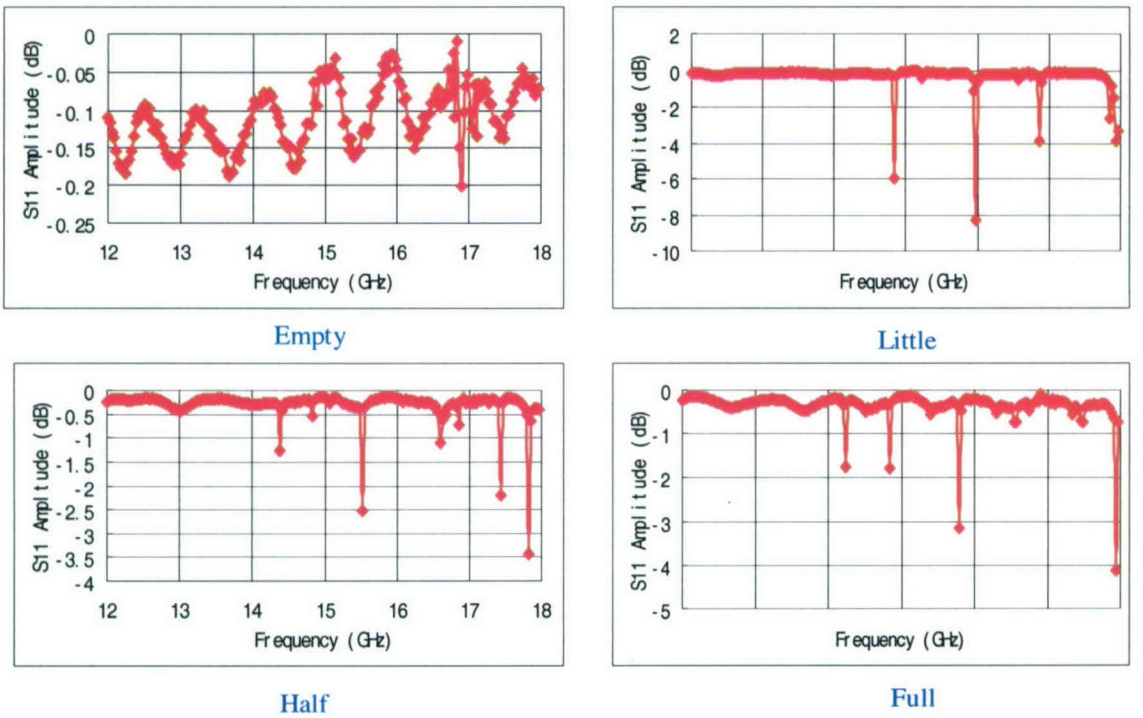

Fig. 9. Ku-Band (12.4-18.0 GHz) one-port (S_{11}) measurements of DPA.

In Fig. 10, we display measurements in K-Band (18-26.5 GHz) of DPA. The sample holder depths are: empty (0 cm), little (0.9 cm), half (3.5 cm) and full (7 cm). As plotted in these figures, we observe no constant-frequency absorptive resonances.

Plotted in Fig. 11 are measurements in Ka-Band (26.5-40 GHz) of DPA. Yet again, the different sample amounts are measured by the sample holder depth: empty (0 cm), little (0.9 cm), and full (6.3 cm). A periodic ripple in the reflected signal amplitude, relatively small in amplitude at the lower frequencies (see Figs. 9,10), is becoming well pronounced at these higher frequencies. The resonances increase in amplitude with sample holder depth, but also shift in frequency indicative not of an absorptive resonance but rather of the presence of multiple spurious reflections. The apparent strength of this interference is due in large part to the difficulty of obtaining a well-matched clean coaxial-to-waveguide transition required by the one port HP 8510 network analyzer. This transition-induced reflection then destructively interferes with reflections from both the air-sample interface as well as the primary sample-short reflection from the bottom of the sample holder.

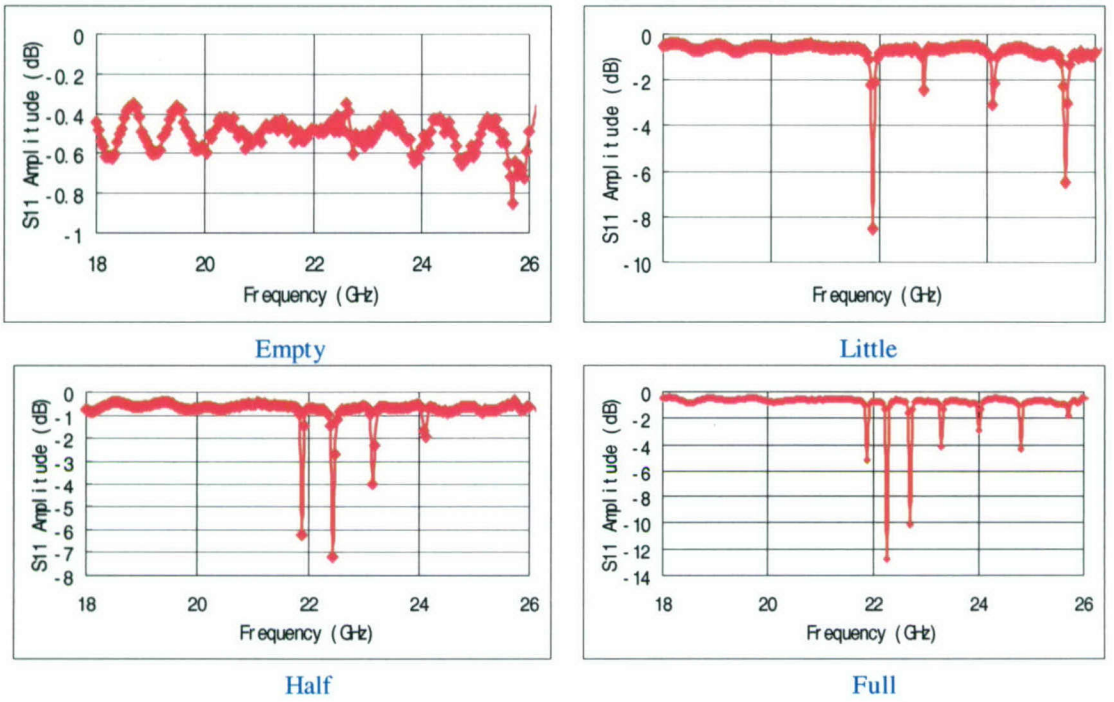

Fig. 10. K-Band (18-26.5 GHz) one-port (S_{11}) measurements of DPA.

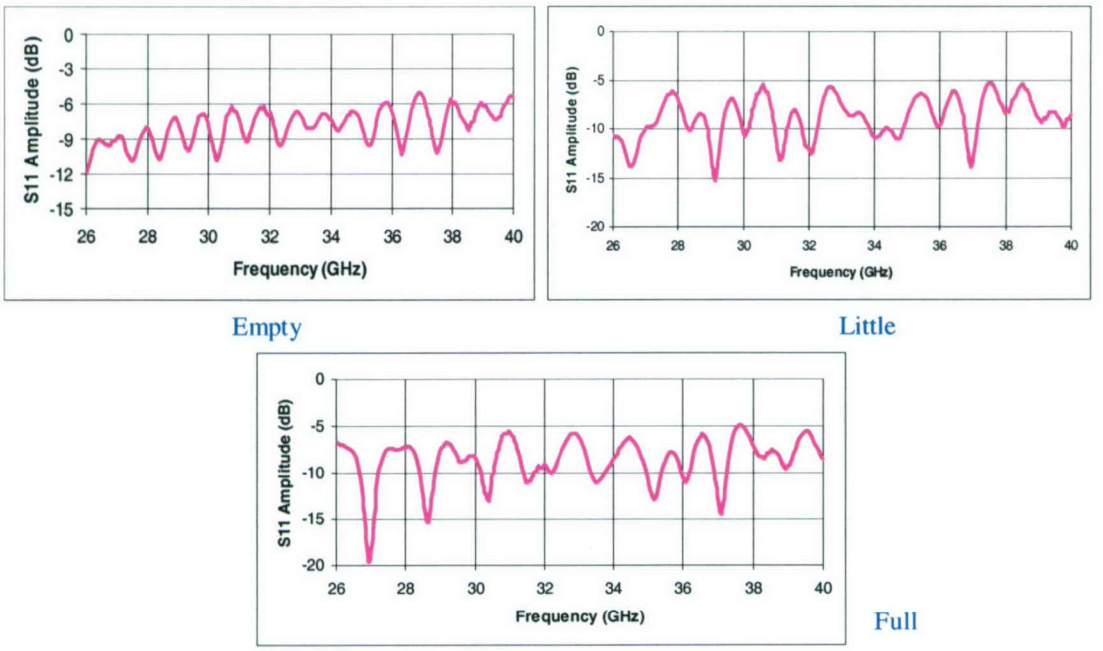

Fig. 11. Ka-Band (26.5-40 GHz) one-port (S_{11}) measurements of DPA.

B.2. Two-Port (S_{21}) Vector Analyzer Data from 26.5 to 40 GHz

Although it is not possible to completely eliminate reflections from the air-sample interface, as discussed in the previous section, the interference effect of the coaxial-to-waveguide transition can be largely avoided by transforming the one-port (S_{11}) measurement into a two-port (S_{21}) measurement. In this configuration, two coaxial-to-waveguide adapters are connected to the coupled and output arms of a 3 dB directional coupler with the input arm of the coupler

connected to the sample holder and short. This is shown in Fig. 12. Here, a thru-reflect-line (TRL) two-port calibration is employed to remove the background attenuation of the directional coupler. In addition, to further reduce the effects of multiple reflections, a waveguide attenuator may be inserted in either the input or output signal paths.

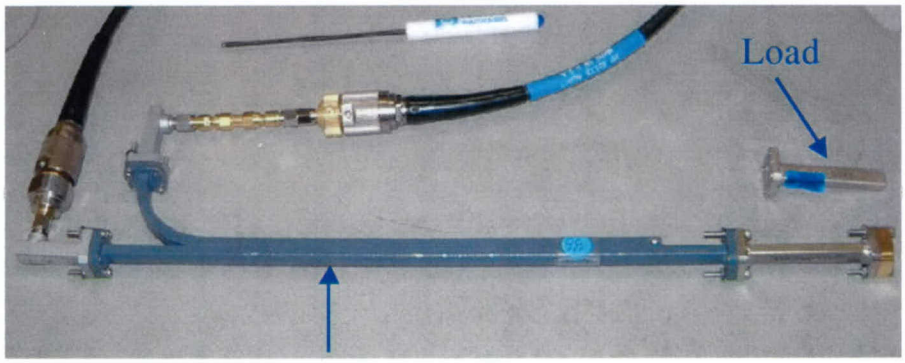

Fig. 12. Photograph of millimeter-wave components employed for two-port dielectric response measurements in Ka Band (26.5-40 GHz).

Plotted in Fig. 13 are measurements in Ka-Band (26.5-40 GHz) of DPA. The different sample amounts are once again measured by their sample holder depth: empty (0 cm), little (1 cm), half (3 cm) and full (6.3 cm). As compared to Fig. 11, the standing wave effects are significantly reduced although not eliminated. Resonances are still observed with DPA present, but with a more constant periodicity indicative of the interference pattern formed by two relatively strong reflections (from the air-DPA interfaces at each end of the sample holder). As the frequency of these resonance valleys changes with the amount of DPA in the sample holder, we conclude the absence of any significant absorptive resonances in this frequency band.

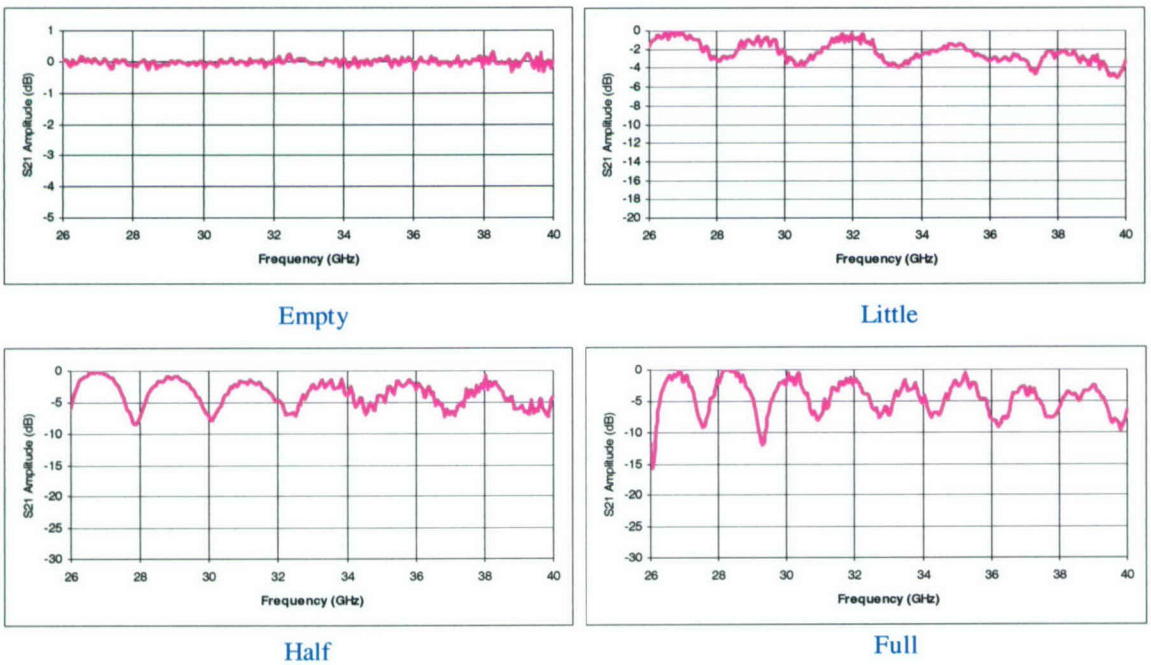

Fig. 13. Ka-Band (26.5-40 GHz) two-port (S_{21}) measurements of DPA.

B.3. Two-Port (S_{21}) Scalar Analyzer Data from 40 to 170 GHz

For measurements above 40 GHz, the HP8510 vector network analyzer may not be employed due to the frequency limitations of the available test sets. Here, a scalar network analyzer configuration is employed. This involves the use of a high frequency source, a millimeter-wave sample holder, and a pair of power sensors or detectors (one to monitor the input power to the sample holder, and one to monitor the power transmitted through the sample holder). Investigations of the spectroscopic resonances of DPA have now been conducted over a frequency range of 40-170 GHz using this technique.

In W-band (75-110 GHz), a synthesized sweeper and broadband multiplier are available for test. This has the advantage of extremely accurate frequency measurement (due to the synthesized sweeper), but the disadvantage of low output power (< 5 mW, due to the X6 multiplier). Directional couplers and power sensors are inserted between the source and the sample to measure the incident and reflected power, while a third sensor placed after the sample measures the transmitted power (see Fig. 14). Here, data are first taken with an empty sample holder, and then with a sample holder with varying amounts of sample present.

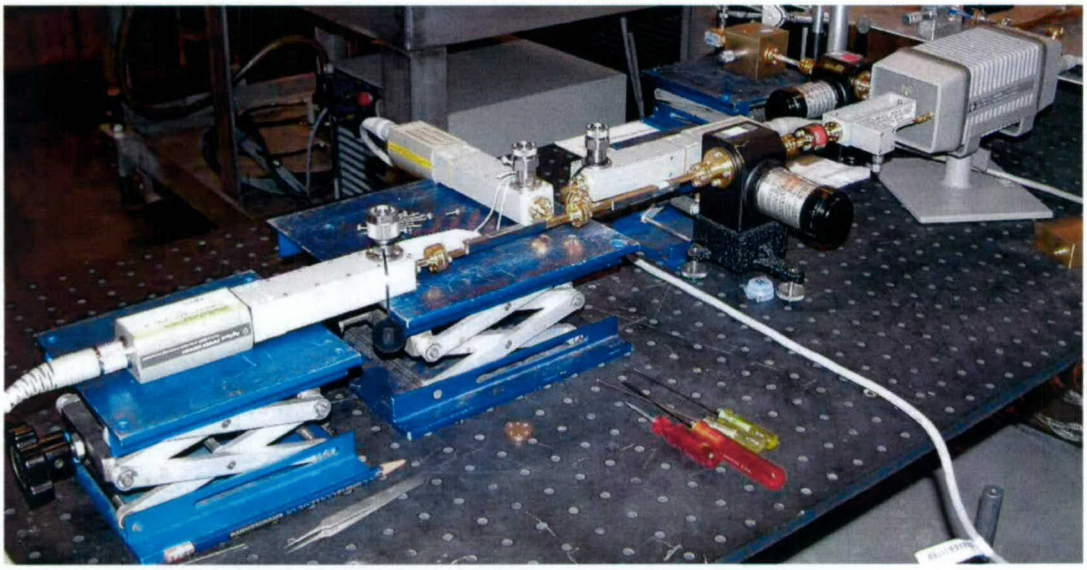

Figure 14. Photograph of the scalar network analyzer setup for W-band (75-110 GHz).

Reflections and standing waves are a recurring problem with these types of waveguide measurements. The presence of the DPA modifies any standing wave patterns that might be present in the test structure. By varying the amount of DPA in the sample holder, the peaks and valleys of the standing wave patterns are shifted in frequency space. Plotting together the measured insertion loss at multiple sample depths, as is done in Fig. 15, allows the actual DPA insertion loss, given by the minimum observed insertion loss of each of the sample depths, to be determined as a function of frequency. From Fig. 15, it can be seen that there are no frequencies between 75 and 115 GHz in which a >1 dB insertion loss is observed.

In the other bands tested, namely Q- (33-50 GHz), U- (40-60 GHz), V- (50-75 GHz), F- (90-140 GHz) and D-bands (110-170 GHz), backward wave oscillator (BWO) sources were used rather than the synthesized sweeper/multiplier source used in W-band (75-110 GHz). Each potential DPA resonance has therefore been retested in a number of different test geometries. We

have found that the best results generally come from the simplest setups coupled with relatively high input and output attenuation settings to reduce input-output standing waves.

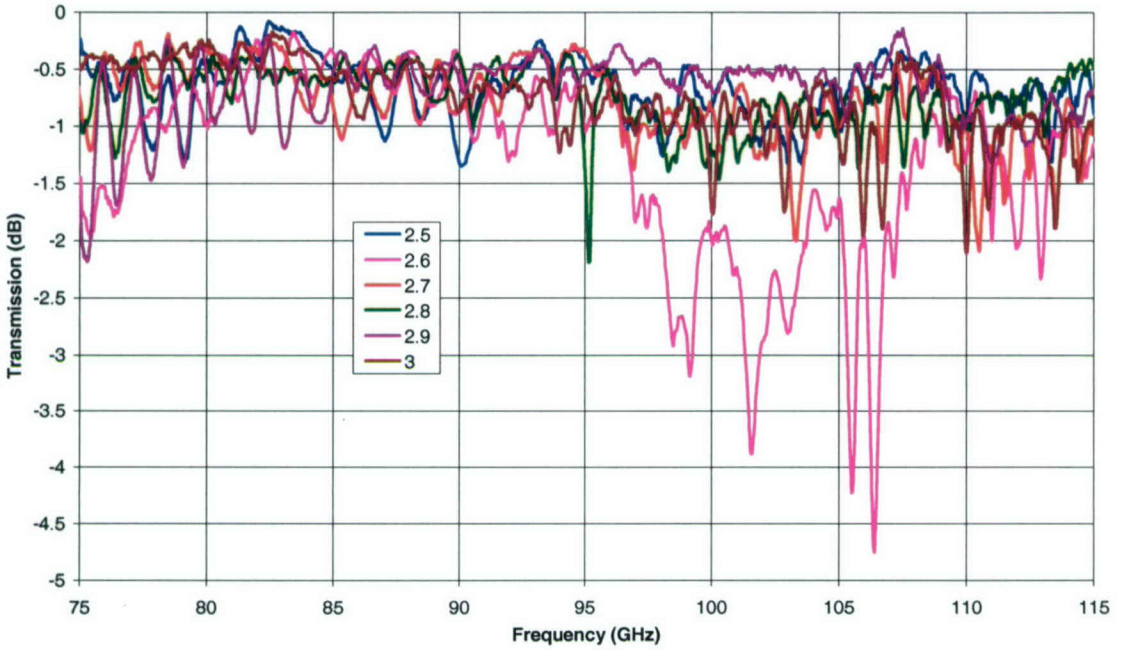

Figure 15. The measured W-Band (75-110 GHz) insertion loss through a 3 inch long sample holder filled with varying depths of DPA ranging from 2.5 to 3.0 inches.

Presented in Fig. 17 are two sets of results obtained with a Q-band sample holder, using a setup similar to that of Fig. 14 but employing a frequency meter to accurately measure the BWO source frequency. High sensitivity square-law detectors are then employed in conjunction with low-noise lock-in amplifiers. In the second data set, shown to the right, the directional coupler and attached frequency meter were taken out of the main line and replaced by a 1" long waveguide section, with a second waveguide section installed immediately before the Q-band sample holder. From these results, it is seen that most if not all of the "resonances" in the left hand data plot arise from interference with reflections from within the 3 dB coupler. With the cleaner experimental setup, no resonances are observed with a >1 dB insertion loss.

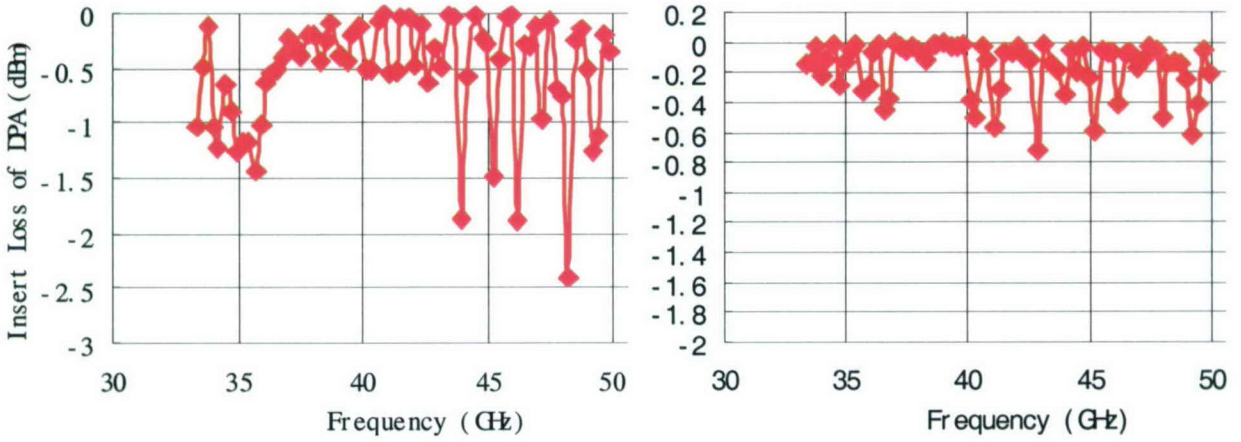

Fig. 17. Q-Band (33-50 GHz) two-port (S_{21}) measurements of DPA.

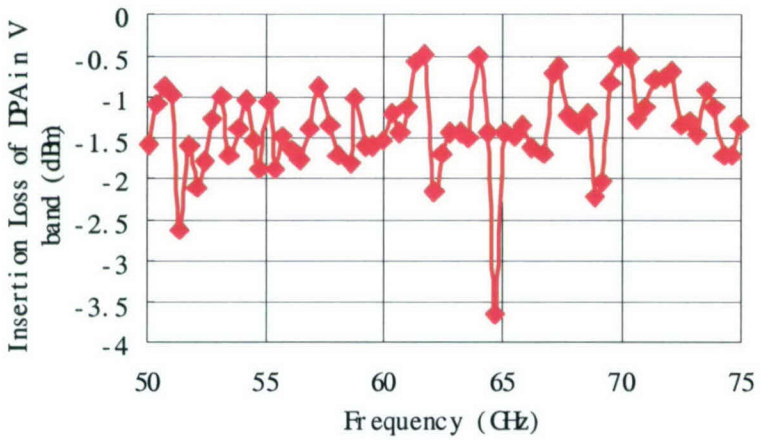

Fig. 18. V-Band (50-75 GHz) two-port (S_{21}) measurements of DPA, showing the transmission loss through a 10.0 cm long sample holder.

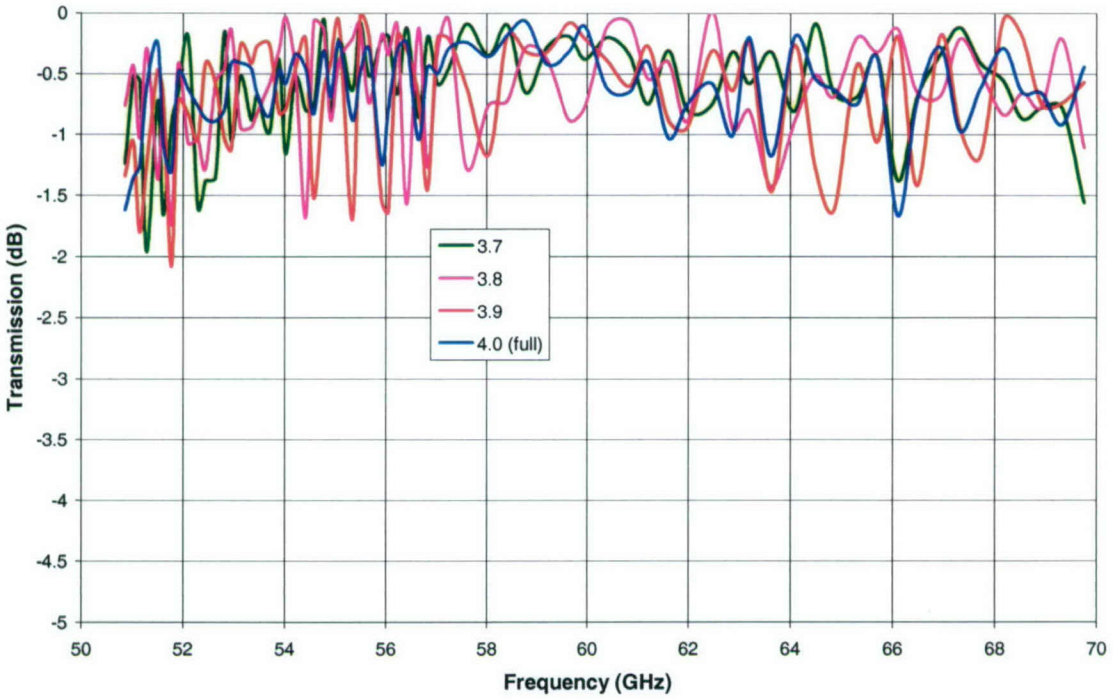

Fig. 19. The measured V-Band (50-75 GHz) insertion loss through a 4.0 inch long sample holder filled with varying depths of DPA ranging from 3.7 to 4.0 inches.

Presented in Fig. 18 and 19 are data obtained with a V-band sample holder. Fig. 18 was taken using high sensitivity square-law detectors are again employed in conjunction with low-noise lock-in amplifiers (see Fig. 20), while Fig. 19 employed power sensors in a semi-automated testing arrangement specifically developed for this program. From the results of Fig. 18, three potential resonances at 51, 65 and 69 GHz are identified. The later measurements of Fig. 19, measuring the transmission through a range of DPA sample depths, demonstrated that these earlier observations were the result of standing waves within testing system. Plotted in Fig. 21 are measurements made with a 6.0 cm long U-band (40-60 GHz) sample holder, using a variety of sample depths ranging from 5.5 to 6.0 cm. We note that the absence of any transmission dips > 1 dB over the 40-55 GHz frequency range tested.

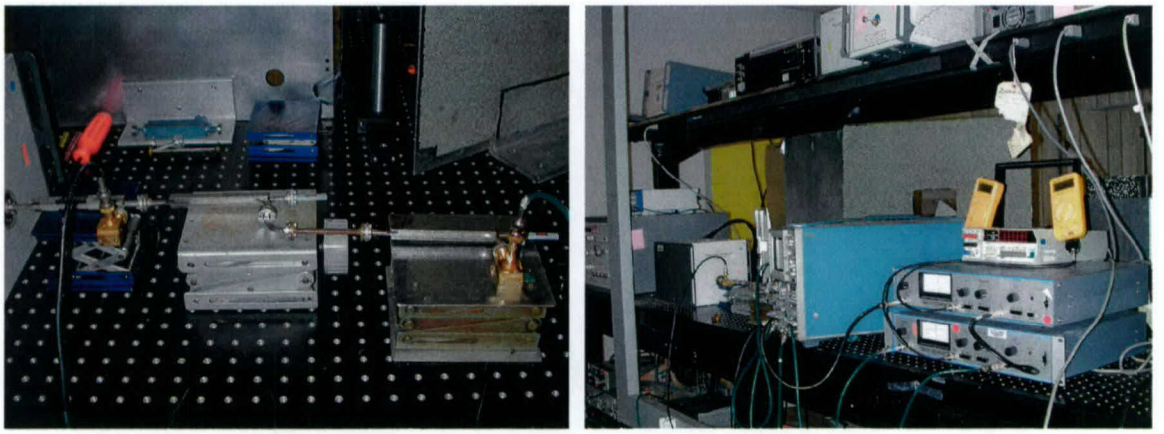

Fig. 20. Photographs of the detector-based V-band (50-75 GHz) network analyzer setup.

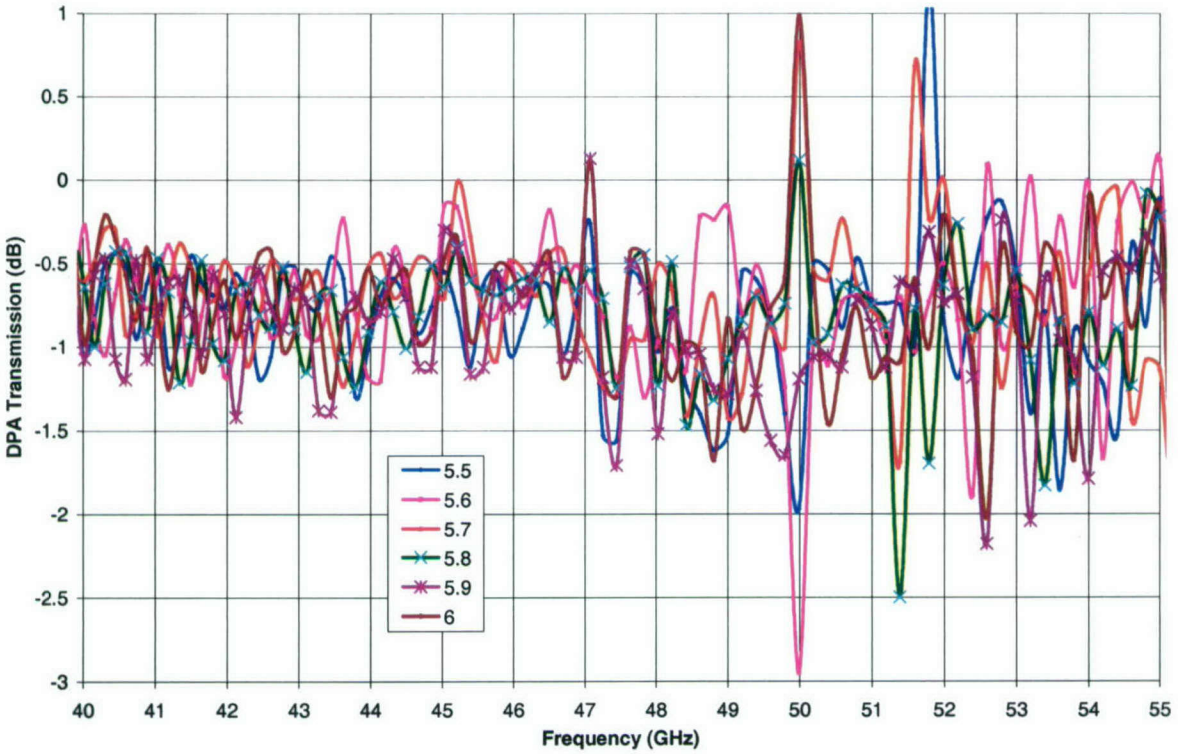

Fig. 21. The measured U-Band (40-60 GHz) insertion loss through a 6.0 cm long sample holder filled with varying depths of DPA ranging from 5.5 to 6.0 cm.

Presented in Fig. 22 are measurements through a 7.5 cm long F-band (90-140 GHz) sample holder, as compared to that of an empty holder. The red curve represents data collected with a power meter-based setup, while the blue curve is more recent data collected with a modified detector-based setup. We note the broad feature observed around 127 GHz, in which the peak transmission falls below 0.7 dB irrespective of the length of the sample holder. To confirm this result, a series of measurements were subsequently performed in D-band (110-170 GHz) with a number of different DPA sample depths. Plotted in Fig. 23 is the transmission through DPA of depths varying from 2.7 to 3.0 inches as compared to the measured transmission through the empty sample holder. Not only is the broad resonance around 127 GHz still present, but additional deeper but broader resonance appears at ~155 GHz. The student will continue to refine

these measurements to more accurately determine the depth and width of the two dielectric resonances. The results of this study will be compiled into a paper to be submitted to *IEEE Microwave and Wireless Components Letters* later this year.

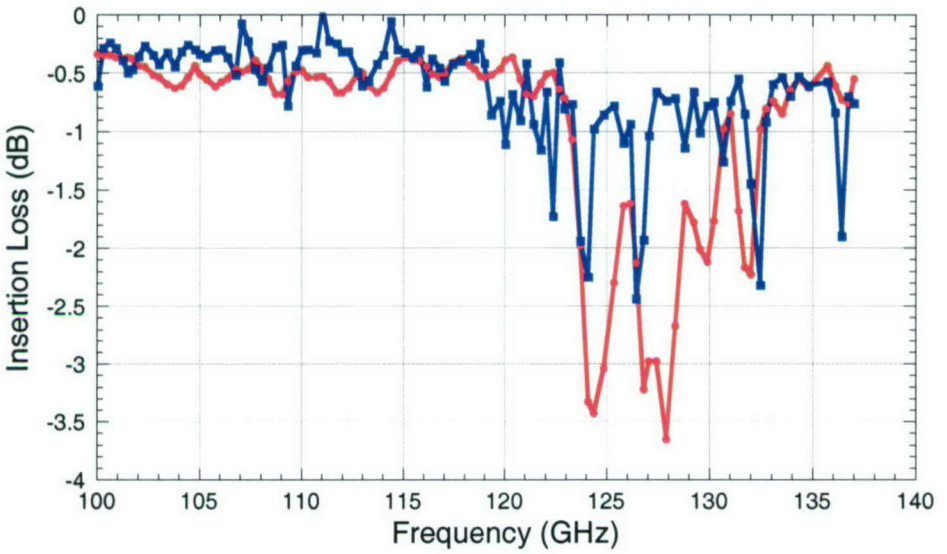

Fig. 22. F-band (90-140 GHz) transmission through a 7.5 cm long sample holder containing DPA; data collected in power-meter-based (-●-) and detector-based (-■-) setups.

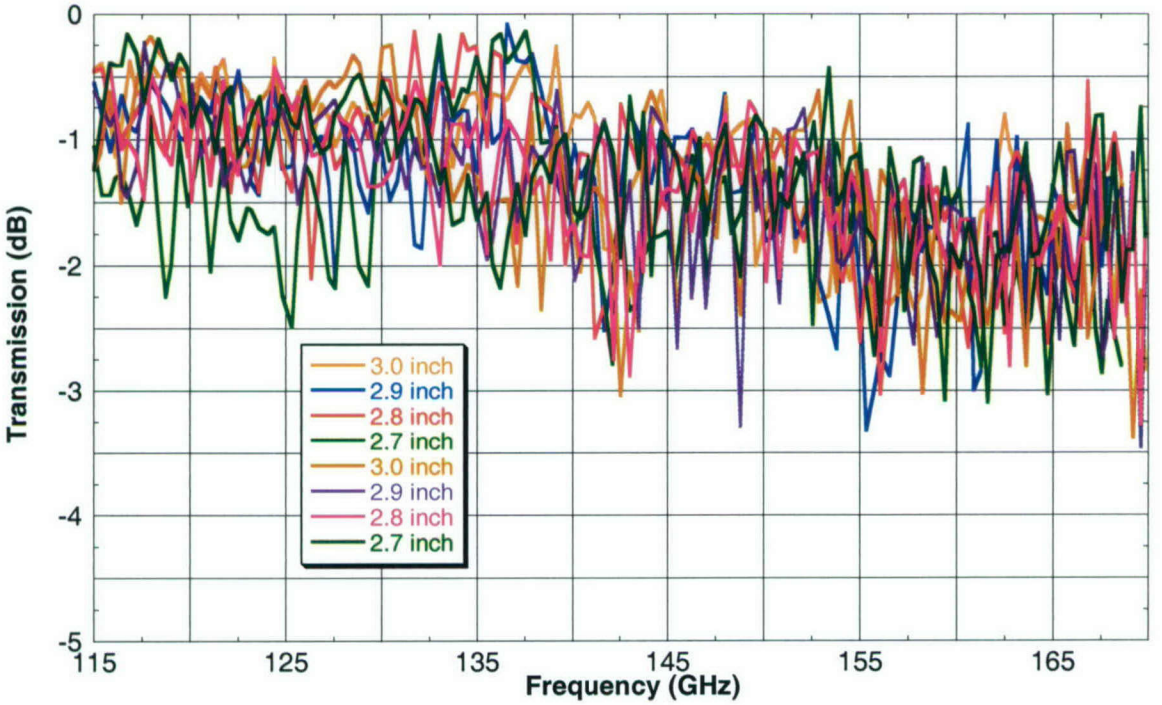

Fig. 23. D-band (110-170 GHz) transmission through a 3 inch long sample holder containing DPA.

C. Liquid Sample Measurements

C.1. Fixture Development

Multi-layered coplanar waveguide (CPW) transmission line structures have been developed for the study of other spore constituents, which are readily available only in small quantities and in liquid suspension. Our approach is based on a technique developed by Signature BioScience, Inc. (now out of business) and reported in Ref. 21 and a similar approach reported in Ref. 22.

Figure 24 contains a schematic illustration of the first of our liquid sample transmission line-based test fixtures, designed for use well beyond the 2.5 GHz frequency limit commercially available. The CPW is fabricated on a custom-designed printed circuit board (PCB), with the liquid (volume ~ 10 microliter) injected between the transmission line and a lexan cover. Measurement data are acquired using an HP8510 vector network analyzer. The liquid sample test fixture is first calibrated with an empty fixture, and then measured with the liquid sample present. The liquid acts to increase the effective dielectric constant (real and imaginary) of the transmission line. The real part is extracted from the S_{21} phase response, while the imaginary (dielectric loss) part is extracted from the S_{21} amplitude. In practice, however, one must model radiation losses as well as dielectric losses in the board and test sample. Simulations of the test sample must be run and optimized to best match the test measurements in order to obtain accurate results.

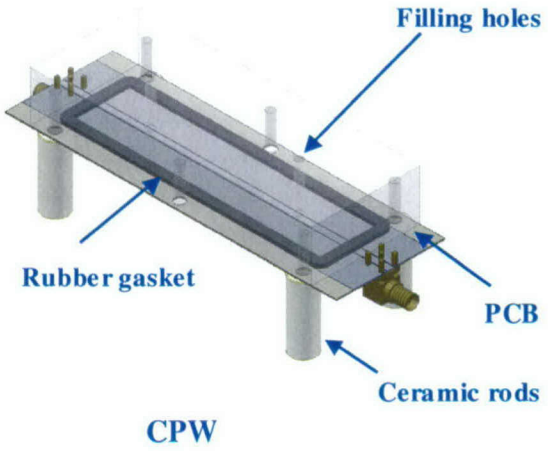

Fig. 24. Illustration of a prototype coplanar waveguide (CPW) structure for use in liquid sample characterization.

Our first test fixtures were limited to use below 7 GHz due to the presence of spurious reflections associated with the SMA input/output connectors placed on the PCB. This situation was later improved with a series of new boards and fixtures using end launch SMA and 2.4 mm connectors rather than the vertical launch used before and illustrated in Fig. 24. Photographs of the final SMA test fixture, together with test results with and without the overlaying lexan liquid sample holder, plotted in Fig. 25. Without the lexan fixture attached, the simple transmission line results show a fairly flat response to about 17 GHz. The presence of the fixture, however, creates reflections and interference patterns that considerably complicate the transmission line response. Care therefore had to be taken to modify the structure of the bottom transmission line so as to yield a flat response with the fixture attached.

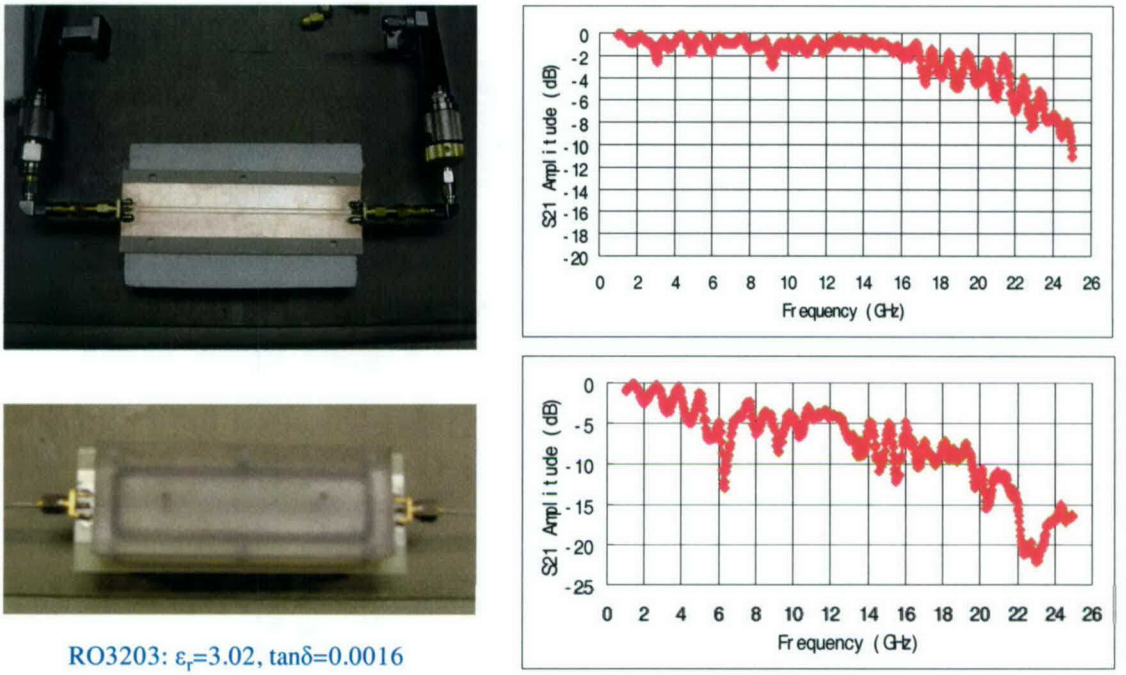

Fig. 25. Measured transmission (S_{21}) results of an end-launch SMA fixture without (above) and with (below) the overlaying liquid sample fixture.

Significantly broader coverage has been achieved through the use of 2.4 mm end launch fixtures. These boards employ a grounded CPW geometry at the end launch connectors for a broadband, low loss interconnect, with transitions to the more conventional CPW lines in the liquid interaction region. Photographs of the new 2.4 mm test fixtures are provided in Fig. 26, while transmission (S_{21}) measurements of the transmission line with and without the lexan liquid sample fixture are plotted in Fig. 27. In comparison to the SMA data of Fig. 25, the 2.4 mm data has exceptionally low loss and clean performance past 35 GHz.

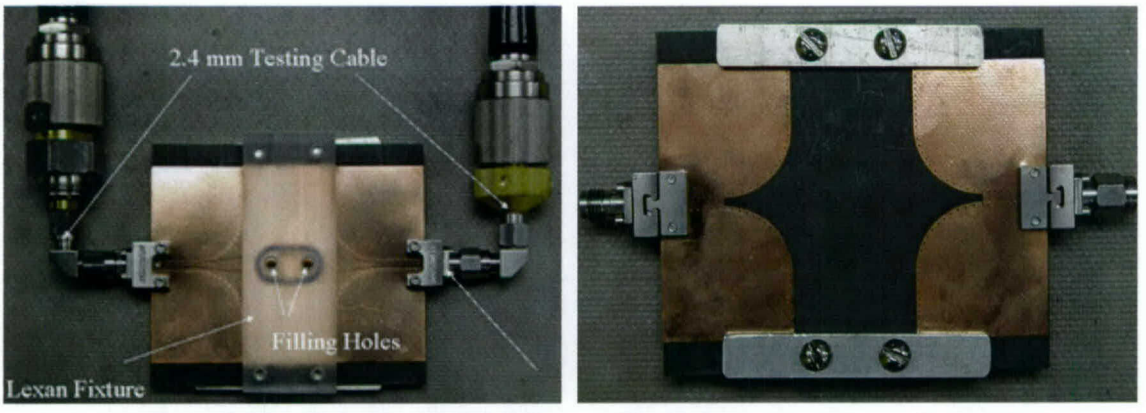

Fig. 26. Top (left) and bottom (right) views of the 2.4 mm liquid sample test fixture.

In preparation to characterizing biological materials in liquid suspension, a number of previously well-characterized liquids were studied in the 2.4 mm test fixture. The first liquid to be tested was isopropyl alcohol. In addition to being one of a number of liquids whose dispersive properties are well known, isopropyl alcohol exhibits relatively low loss over this frequency range. Plotted in Fig. 28 are the measured S-parameter data for isopropyl alcohol (99% purity).

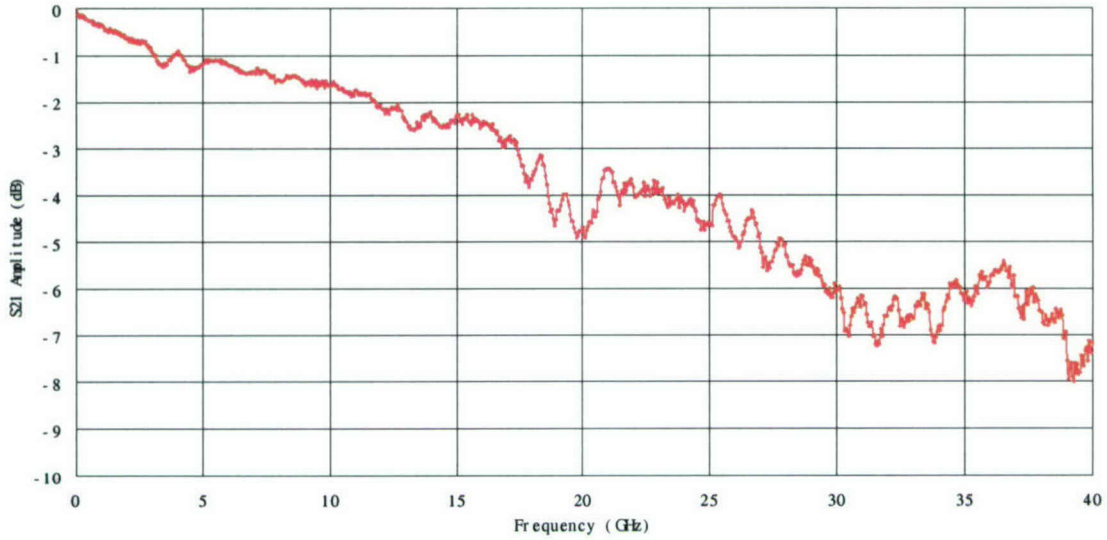

Fig. 27. Measured transmission (S_{21}) characteristics of the 2.4 mm CPWG test fixture.

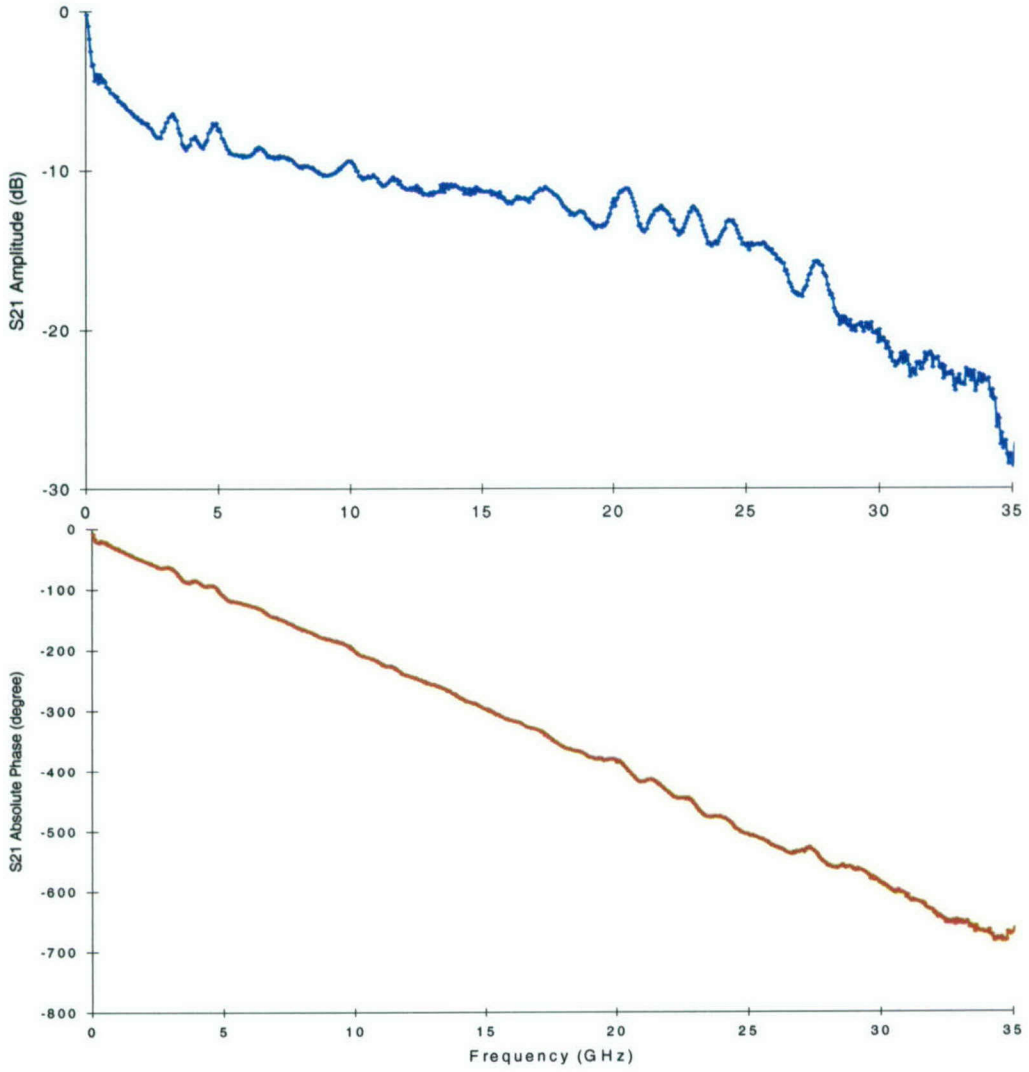

Fig. 28. Measured S-parameters of isopropyl alcohol (99% pure).

The S_{21} transmission data are then inverted to yield the effective dielectric constant of isopropyl alcohol as shown below in Fig. 29. The data compare well with published data from Agilent Technologies, reproduced in Fig. 30. Here, we have assumed that the height of the liquid in the sample holder is much greater than the thickness of the board itself, so that we can more easily approximate the CPW line impedance. More recently, our Ph.D. student has begun work on modeling the test fixture in order to better extract the dielectric parameters of the test sample. Here, the circuit is divided into a number of regions as shown in Fig. 31. Using these models, we have simulated the test structure using the IE3D simulator program. Plotted in Fig. 32 are simulation results using ethanol, another of the well established test liquids whose dielectric properties are well understood, plotted against the theoretical results (from relaxation theory) and experimental measurements taken with the test fixture of Fig. 24).

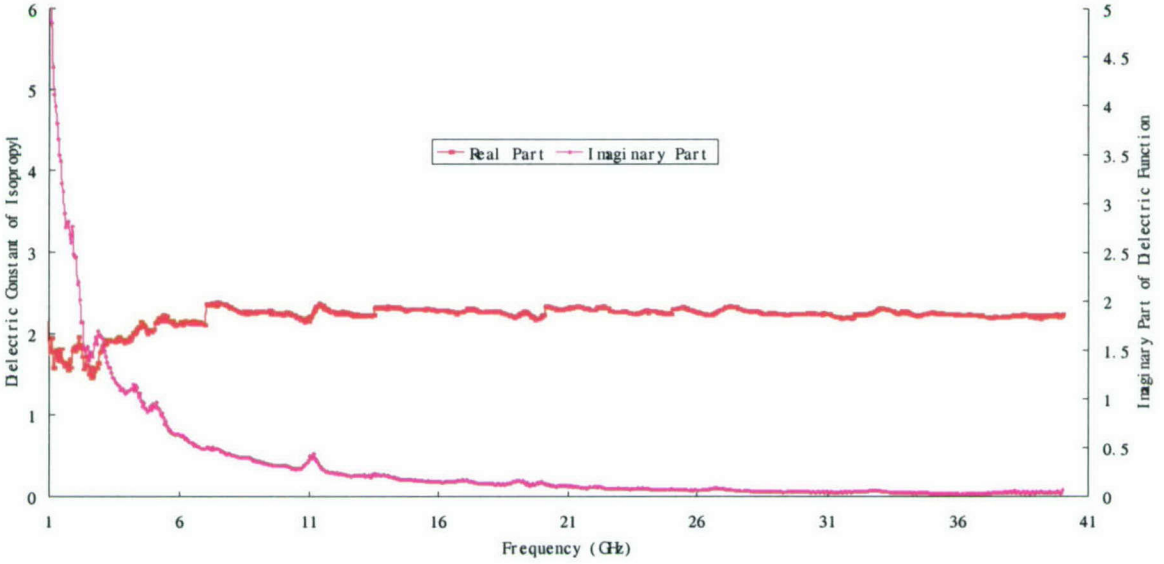

Fig. 29. Dielectric constant of isopropyl alcohol, as extracted from measured data of Fig. 28.

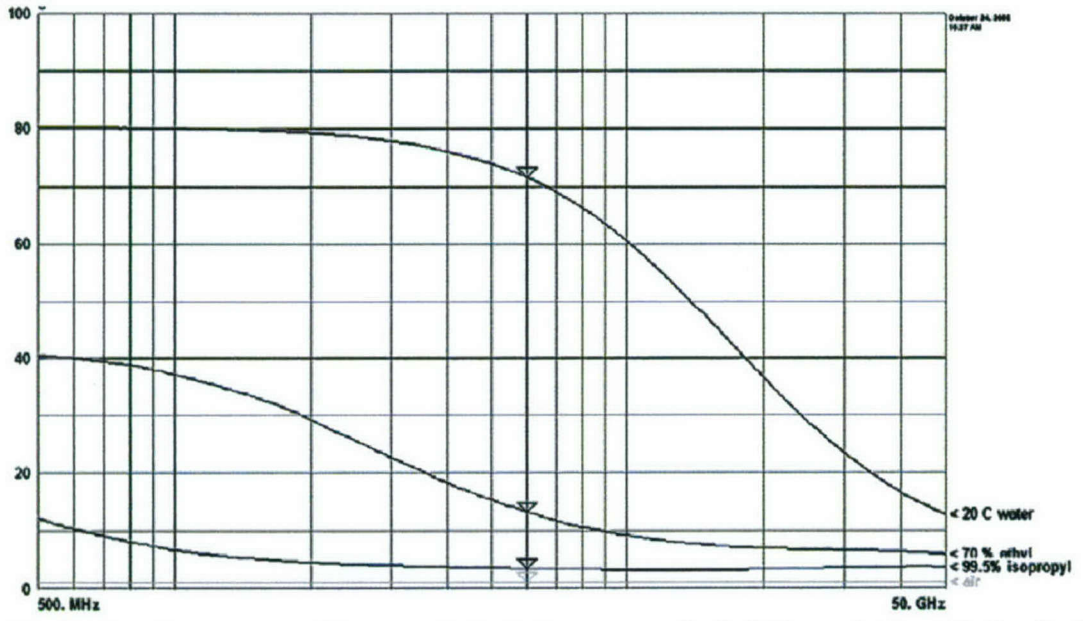

Fig. 30. Dielectric constant of isopropyl alcohol, water and ethyl (from Agilent Technologies).

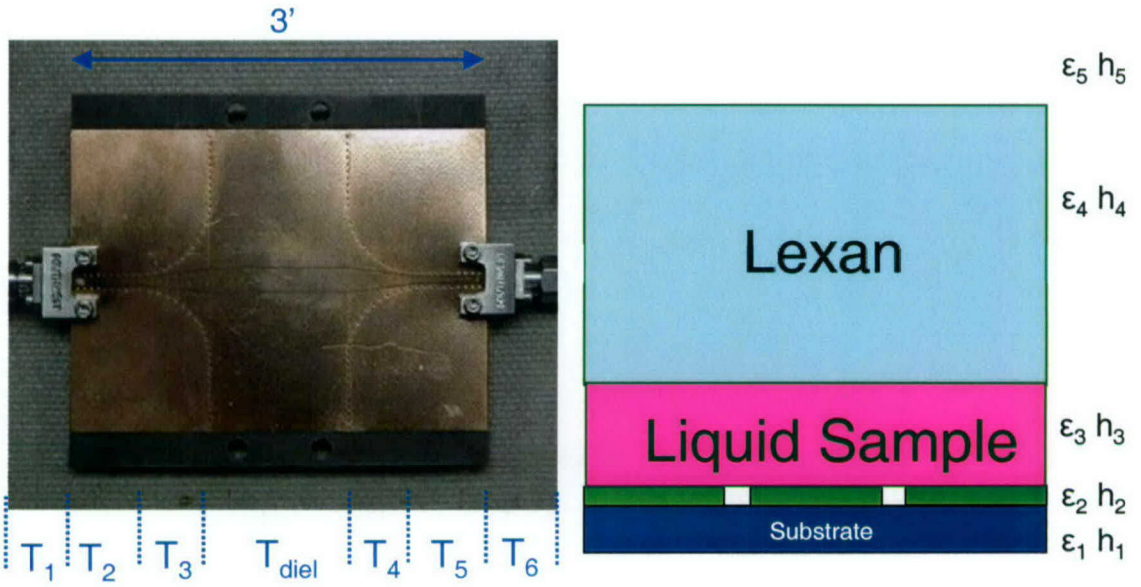

Fig. 31. Matrix representation of the liquid sample measurement cell (left), and corresponding cross-section of the multilayered CPW structure in the cell center (right).

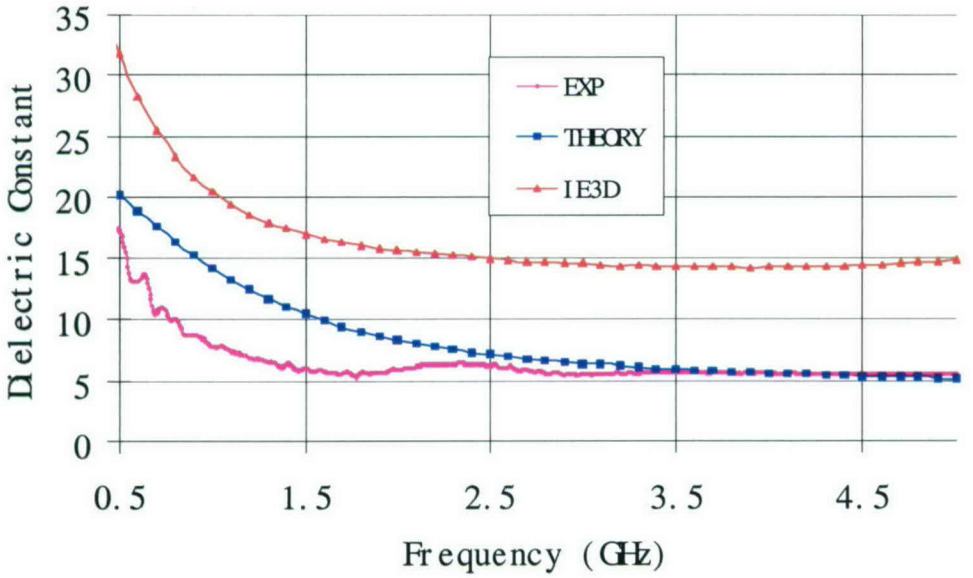

Fig. 32. Dielectric constant calculations of ethanol determined experimentally, using relaxation theory, and simulated using the IE3D simulator.

C.1. Buffer Liquid Investigations

A significant difficulty that needs to be overcome in characterizing biological materials in liquid suspension is the inherent loss of the water-based buffer solutions that the materials are embedded. Plotted in Fig. 33 are measured transmission data of a solution of 0.25 M Tris buffer (pH = 8) placed within the liquid sample holder. As can be clearly seen, the transmission loss increases rapidly to > 40 dB at ~4 GHz, above which the measurement data suffer from poor signal-to-noise ratios. The focus here is thus to identify alternate buffer liquids with low loss performance at microwave and millimeter-wave frequencies. One potential candidate is 3M

fluorinert electronic liquid FC-75, which is commonly employed as a cooling liquid in microwave applications to enhance heat transfer away from critical system components. Transmission data of FC-75, plotted in Fig. 34, shows extremely low loss performance up past 40 GHz (the maximum frequency that can be probed with our HP 8510 vector network analyzers).

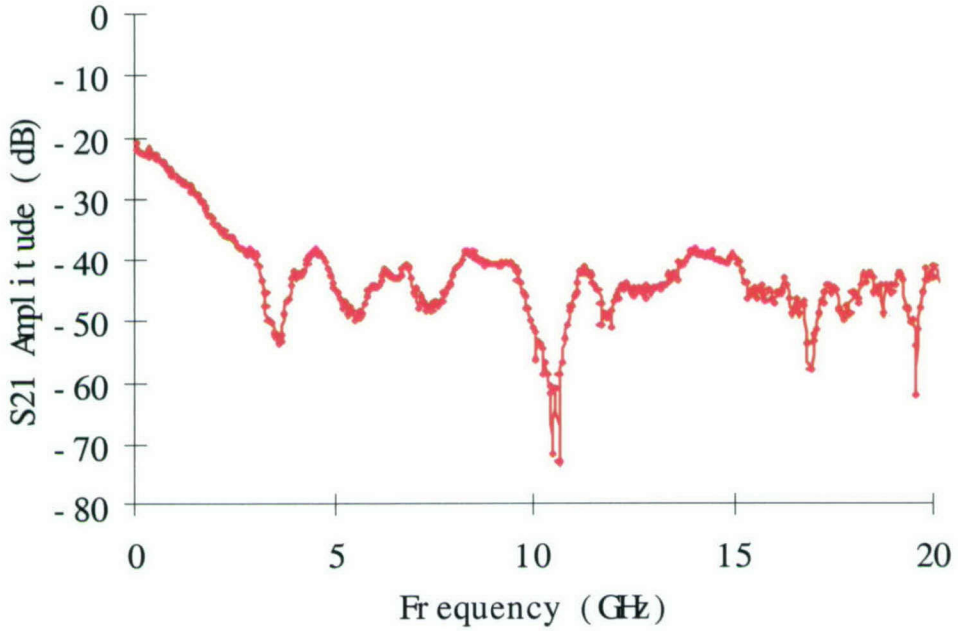

Fig. 33. Measured transmission (S_{21}) loss of the 2.4 mm test fixture filled with 0.25 M Tris buffer (pH = 8) solution.

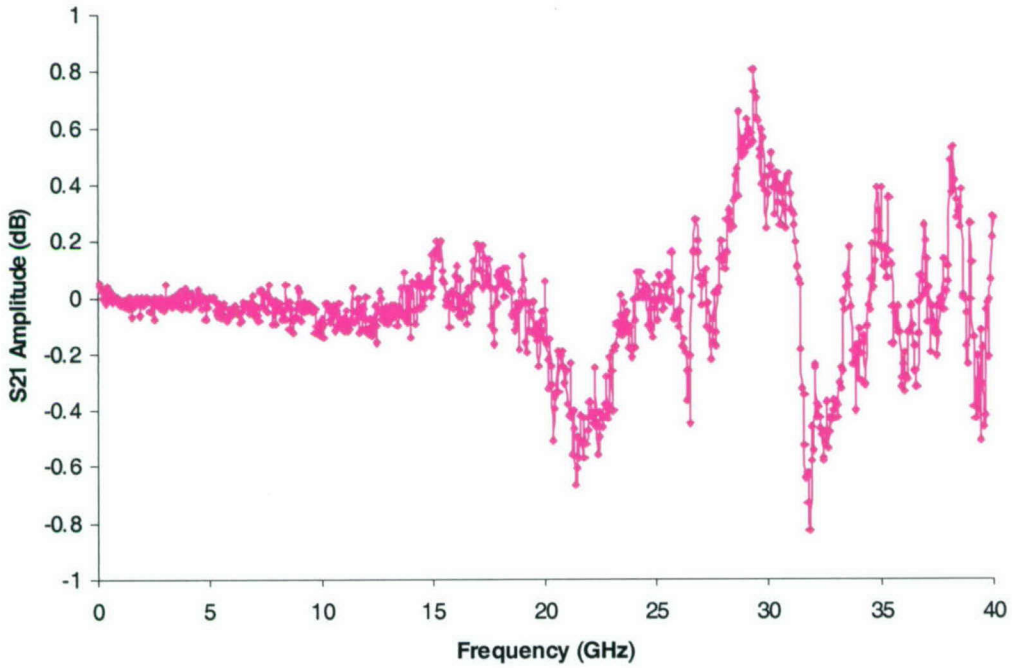

Fig. 34. Measured transmission (S_{21}) loss of the 2.4 mm test fixture filled with 3M fluorinert electronic liquid FC-75.

IV. References

1. P. Debye, *Polar Molecules*, Lancaster, Lancaster Press (1929).
2. S.A. Goldblith and D.I.C. Wang, "Effect of Microwaves on Escherichia coli and Bacillus Subtilis," *J. Applied Microbiol.* **15**, pp. 1371-1375 (1967).
3. P.V. Brown, R.H. Lenox and J.L. Meyerhoff, "Microwave Enzyme Inactivation System: Electronic Control to Reduce Dose Variability." *IEEE Transactions on Biomedical Engineering* **2**, pp. 205-208 (1978).
4. M.R. Sanborn, S.K. Wan and R. Bulard (1982), "Microwave Sterilization of Plastic Tissue Culture Vessels for Reuse," *Applied and Environ. Microbiol.* **44**, pp. 960-964 (1982).
5. Welt, B. A., C. H. Tong, J. L. Rossen and D. B. Lund (1994). "Effect of microwave radiation on inactivation of Clostridium sporogenes spores." Applied and Environ. Microbiol. 60: 482-488.
6. A. Vaid and A.H. Bishop, "The Destruction of Microwave Radiation ofy Bacterial Endospores and Amplification of the Released DNA," *J. Applied Microbiol.* **85**, pp. 115-122 (1998).
7. D.K.H. Jeng, K.A. Kaczmarek, A.G. Woodworth and G. Balasky, "Mechanism of Microwave Sterilization in the Dry State," *Applied and Environ. Microbiol.* **53**, pp. 2133-2137 (1987).
8. Y. Kakita, N. Kashige, K. Murata, A. Kuroiwa, M. Funatsu and K. Watanabe, "Inactivation of Lactobacillus Bacteriophage PL-1 by Microwave Irradiation," *Microbiol. Immunol.* **39**, pp. 571-576 (1995).
9. H. Fujikawa, H. Ushioda and Y. Kudo, "Kinetics of Escherichia coli destruction by microwave irradiation," *Applied and Environ. Microbiol.* **58**, pp. 920-924 (1992).
10. Y. Kakita, M. Funatso, F. Miake, and K. Watanabe, "Effects of Microwave Irradiation on Bacteria Attached to the Hospiral White Coats," *Int. J. of Occup. Med. & Environ. Health* **12**, pp. 123-126 (1999).
11. V.K. Saxena, B.H. Dorfman, L.L. Van Zandt, *Physical Review A* **43**, 4510 (1991).
12. J. Ju, H-L. Cui, A.C. Samuels, J. Jensen, D. Woolard, "Millimeter Wave Absorption Spectroscopy of Biopolymers," *Proc. SPIE* **4574**, pp. 129-136 (2001).
13. J. Ju, "Millimeter Wave Absorption Spectroscopy of Biological Polymers," *Ph.D. Thesis – Stevens Institute of Technlogy* (2001).
14. D.L. Woolard, R. Kaul, R. Suenram, A.H. Walker, T. Globus, A. Samuels, *IEEE MTT-S Int. Microwave Symp. Dig* **3**, 925 (1999).
15. D.L. Woolard, T.R. Globus, B.L. Gelmont, M. Bykhovskaia, A.C. Samuels, D. Cookmeyer, J.L. Hesler, T.W. Crowe, J.O Jensen, J.L. Jensen, W.R. Loerop, *Physical Review E* **65**, 051903 (2002).
16. T. Globus, D. Woolard, M. Bykhovskaia, B. Gelmont, L. Werbos, and A. Samuels, "THz Frequency Spectroscopic Sensing of DNA and Related Biological Materials," *Int J. of High Speed Electronics and Systems* **13**, pp. 903-936 (2003).
17. T.R. Globus, D.L. Woolard, T. Khromova, T.W. Crowe, M. Bykhovskaia, B.L. Gelmont, J. Hesler, A.C. Samuels, *J. Biol. Phys* **29**, 89 (2003).

18. T. Globus, M. Bykhovskaia, D. Woolard, D. Gelmont, *J. Phys. D* **36**, 1314 (2003).

19. E.R. Brown, "Fundamentals of Terrestrial Millimeter-Wave and THz Remote Sensing," *Int J. of High Speed Electronics and Systems* **13**, pp. 995-1097 (2003).

20. E.R. Brown, J.E. Bjarnason, T.L.J. Chan, A.W.M. Lee, M.A. Celis, "Optical Attenuation Signatures of Bacillus Subtillus in the THz Region," *Applied Physics Letters* **84**, pp. 3438-3440 (2004).

21. J. Hefti, A. Pan and A. Kumar, "Sensitive Detection Method of Dielectric Dispersions in Aqueous-Based, Surface-Bound Macromolecular Structures using Microwave Spectroscopy," *Applied Physics Letters* **75**, pp. 1802-1804 (1999).

22. G.R. Facer, D.A. Notterman and L.L. Sohn, "Dielectric Spectroscopy for Bioanalysis: From 40 Hz to 26.5 GHz in a microfabricated wave guide," *Applied Physics Letters* **78**, pp. 996-998 (2001).